CT&F Ciencia, Tecnología y Futuro
ISSN: 0122-5383
ctyf@ecopetrol.com.co
ECOPETROL S.A.
Colombia

López-Ramos, Eduardo
HYDROCARBON GENERATION MODELS ALONG THE BASAL DETACHMENT OF THE ANDEAN SUBDUCTION ZONE IN NORTHERN ECUADOR TO SOUTHERN COLOMBIA
CT&F Ciencia, Tecnología y Futuro, vol. 6, núm. 3, junio, 2016, pp. 25-51
ECOPETROL S.A.
Bucaramanga, Colombia

Available in: http://www.redalyc.org/articulo.oa?id=46549474002

CT&F - Ciencia, Tecnología y Futuro - Vol. 6 Num. 3 Jun. 2016 Pag. 25 - 52

JOURNAL
CIENCIA, TECNOLOGÍA Y FUTURO
ctyf

ISSN (Print) 0122-5383
ISSN (Online) 2382-4581
Journal of oil, gas and alternative energy sources

HYDROCARBON GENERATION MODELS ALONG THE BASAL DETACHMENT OF THE ANDEAN SUBDUCTION ZONE IN NORTHERN ECUADOR TO SOUTHERN COLOMBIA

MODELOS DE GENERACIÓN DE HYDROCARBUROS A LO LARGO DEL DESPEGUE BASAL DE LA ZONA DE SUBDUCCIÓN ANDINA EN EL NORTE DE ECUADOR Y SUR DE COLOMBIA

MODELOS DE GERAÇÃO DE HIDROCARBONETOS AO LONGO DO DEPRESSÃO BASAL DA ZONA DE SUBDUCÇÃO ANDINA NO NORTE DO EQUADOR E SUL DA COLÔMBIA

Eduardo López-Ramos[1]*

[1] Ecopetrol S. A., Vicepresidencia de Exploración, Bogotá, Cundinamarca, Colombia

e-mail: eduardo.lopezra@ecopetrol.com.co

(Received: Sep. 22, 2014; Accepted: Jun 01, 2016)

ABSTRACT

Numerous fluid vents and hydrocarbon seeps of a thermogenic origin have been reported in the middle and lower slope of the Northern Ecuadorean - Southern Colombian (NESC) Pacific margin. These hydrocarbon manifestations are frequently located over the traces of faults connected with the basal detachment of the subduction zone, very far (80km) from the hydrocarbon kitchens formed along the axis of the NESC forearc basins. In some subduction zones, the origin of these types of thermogenic seeps is related to the generation and migration of hydrocarbons along the subduction zone décollement. To test the possibility of generation of hydrocarbons in the NESC décollement, 2D Time-Temperature Index Arrhenius equation (TTIArr) numerical models were constructed in four regional cross sections. The results suggest that along the top of the subducting plate, favorable conditions exist for oil and gas generation below depths of 10 km , with subtle variations of the oil and gas depths of generation, due to lateral changes in the thermal structure of the margin. The available geophysical data support the presence of favorable structures to trap the hydrocarbons generated along the top of the subducting plate (low velocity zones), and/or the seepage of fluids to the sea floor along the middle and lower slope of the NESC margin.

Keywords: *Subduction plane, Hydrocarbons, 2DTTIArr, Low velocity zones.*

How to cite: López-Ramos, E., (2016). Hydrocarbon generation models along the basal detachment of the andean subduction zone in northern ecuador to southern colombia. *CT&F - Ciencia, Tecnología y Futuro*, 6(3), 25 - 52.

**To whom correspondence should be addressed*

RESUMEN

Numerosos orificios de líquido y filtraciones de hidrocarburos de origen termogénico se han reportado en la parte media y baja del talud de la margen Norecuatoriana - Surcolombiana (NESC). Estas manifestaciones se encuentran con frecuencia sobre los trazos de las fallas relacionadas con el plano de subducción, muy lejos de las cocinas de hidrocarburos formadas a lo largo del eje de las cuencas de antearco. En algunas zonas de subducción el origen de este tipo de manifestaciones están relacionadas con procesos de generación y migración de hidrocarburos en el plano de subducción. Para probar la posibilidad de generación de hidrocarburos en el plano de subducción NESC, se construyeron modelos 2D Time-Temperature Index Arrhenius equation (TTIArr) en cuatro secciones regionales. Los resultados sugieren que en el plano subducción existen las condiciones para la generación de petróleo y gas por debajo de 10 km de profundidad, con sutiles variaciones debido a cambios laterales en la estructura térmica del margen. Los datos geofísicos disponibles apoyan la presencia de estructuras favorables para retener los hidrocarburos generados en el plano de subducción (zonas de baja velocidad, cuña de acreción) o su escape al fondo del mar, en la parte media y baja del talud del margen NESC.

Palabras clave: *Plano de subducción, Hidrocarburos, 2DTTIArr, Zona de baja velocidad.*

RESUMO

Numerosos orifícios de líquido e filtrações de hidrocarbonetos de origem termogênica foram verificados na parte média e baixa do talude da margem Nor-equatoriana – Sul-Colombiana (NESC). Estas manifestações são encontradas frequentemente sobre os traços das falhas relacionadas com o plano de subducção, muito longe das cozinhas de hidrocarbonetos formadas ao longo do eixo das bacias do antearco. Em algumas zonas de subducção a origem deste tipo de manifestações estão atreladas a processos de geração e migração de hidrocarbonetos no plano de subducção. Para testar a possibilidade de geração de hidrocarbonetos no plano de subducção NESC, construíram-se modelos de equações 2D Time-Temperature Index Arrhenius (TTIArr) em quatro seções regionais. Os resultados sugerem que no plano de subducção existem as condições para a geração de petróleo e gás por debaixo de 10 Km de profundidade, com sutis variações por conta de mudanças laterais na estrutura térmica da margem. Os dados geofísicos disponíveis apoiam a presença de estruturas favoráveis para reter os hidrocarbonetos gerados no plano de subducção (zonas de baixa velocidade, cunha de acrescimento) ou seu escape para o fundo do mar, na parte média e baixa do talude da margem NESC.

Palavras-chave: *Plano de subducção, Hidrocarbonetos, 2DTTIArr, Zona de baixa velocidade.*

1. INTRODUCTION

Numerous subduction zones worldwide have been drilled by International Ocean Discovery Program (IODP) and Deep Sea Drilling Program (DSDP) missions that gathered evidence of hydrocarbons in the form of gas, oil and bitumen along their lower and middle slopes (Watkins *et al*. 1981; von Huene *et al*. 1982; von Huene *et al*. 1977; Westbrook *et al*. 1994; Kimura *et al*. 1997; Behrmann *et al*. 1992; Taira *et al*. 1991). Part of these hydrocarbons have a thermogenic origin, resulting from the progressive increase in pressure and temperature conditions imposed on the subducting sediments with lesser quantities of organic matter lower than to 2% of TOC (Kvenvolden and von Huene, 1985). Despite the low TOC values in sediments into the subduction zones, the scale of the hydrocarbon generation is prodigious (during the Phanerozoic alone, this process may have generated 1000 times more hydrocarbons than those now present in known reserves of oil and gas), but the mechanism of preservation is extremely inefficient and poorly understood (Areshev and Balanyuk, 2006). The few models of generation of thermogenic hydrocarbons along subduction zones show that the oil and gas generation window occurs at depths that exceed 10 km, strongly controlled by the convergence velocity and thermal structure of the margin (Lutz *et al*., 2004). It is worth noting that the understanding of the conditions of generation of hydrocarbons in the basal detachment remains poorly understood, despite the several manifestations of gases and oils with thermogenic origin recovered from samples of wells drilled along Costa Rica, Nicaragua and Aleutians trenches (Lutz *et al*., 2004, Jefffrey *et al*., 1982, von Huene *et al*., 1982; Kvenvolden and von Huene, 1985).

During the last two decades, the use of wide angle seismic information and new processing techniques in the study of convergent margins with evidence of great earthquakes has provided good seismic images and velocity models of the subduction zone crustal structure in the Nankai Trough (Dessa *et al*. 2004; Kodaira *et al*. 2005), Costa Rican subduction zone (Christeson *et al*. 1999), Chilean subduction zone (Sallarès and Ranero, 2005) and the southwestern Colombian margin (Collot *et al*. 2008; Agudelo *et al*. 2009; García – Cano *et al*. 2014). This information has been fundamental to understand the conditions and mechanism of fluid expulsion along the basal decollement (Hensen *et al*. 2004), alteration processes of the overriding plate (Collot *et al*., 2008; von Huene *et al*, 2004) and tectonic erosion mechanisms (Ranero and von Huene, 2000; Sage *et al*. 2006). Nevertheless, the knowledge of the processes of generation, migration, entrapment and escape of hydrocarbons in subduction zones remains poorly understood. Also, the relation between the hydrocarbon generation and the type of subduction (tectonic accretion or erosion), the quantity of sediments being subducted and changes in the thermal structure is often undetermined.

In order to understand the probable conditions of hydrocarbon formation, their migration in subduction zones and the impact that the type of subduction has over the development of potential petroleum systems, we conducted a regional study of the North Ecuadorean/ Southern Colombian Pacific margin (NESC). To develop our study of the NESC margin we used previously published data including 2D and 3D wide angle seismic data (Agudelo *et al*., 2009; Collot *et al*., 2008; García – Cano *et al*., 2014), evidence of thermogenic oil, gas and fluids near the subduction zone (López, 2009; ANH, 2014), thermal structure variations (Marcaillou *et al*. 2006; Marcaillou *et al*. 2008), and changes in the type of margin and thickness of sediment in subduction (Sage *et al*. 2006; Marcaillou *et al*. 2006a). All information was integrated in regional cross sections used to build 2D numerical models of the *TTIArr* (Time Temperature Index based on the Arrhenius equation) along the top of the subducting plate. The results of the 2D models were compared to understand the variations of the depth in the hydrocarbons kitchens as a function of the thermal structure and subduction type.

2. GEOLOGICAL SETTING

The subduction zone of the NESC margin (Figure 1) is the result of the slightly oblique convergence between the Nazca Plate and the South American Plate at rates of 54 to 58 mm/y (Kendrick *et al*. 2003; Trenkamp *et al*. 2002). Due to this convergence, the Nazca Plate subducts below the South American Plate along the Ecuadorean – Colombian subduction zone (Figure 1). The overriding South American Plate from the Gulf of Guayaquil in Ecuador to Northwestern Colombia consists of oceanic terrains accreted onto the South American continent (Case *et al*. 1973; Aspden and

Litherland, 1992) during the Mesozoic and Cenozoic times (McCourt *et al*. 1984; Cediel *et al*. 2003). Geochemical and geochronological data show that the accreted oceanic terrains are composed primarily of Mid-Ocean Ridge Basalts (MORBs) and island arcs rocks (Barrero, 1979; McCourt *et al*. 1984; Spadea and Spinoza, 1986) or oceanic plateau fragments covered by a calco-alkaline volcano-sedimentary complex and toleiitic island arcs (Reynaud *et al*. 1999; Kerr *et al*. 2002). Wide angle seismic information integrated with gravimetric data confirms the oceanic affinity of the basement along the NESC margin (Case *et al*. 1973; Meyer *et al*. 1977; Agudelo, 2005; Collot *et al*. 2008). The values of the p-wave velocities obtained from seismic refraction data show that at depths greater than 10 km the basement has properties of a lower crust oceanic plateau (Collot *et al*. 2008; Agudelo *et al*. 2009). In some areas, the basement of the NESC margin has subsided more than 10 km allowing the formation of the thick sedimentary Tumaco basin (Case *et al*. 1973; Meissnar *et al*. 1976) and other minor basins such as the Manglares basin, that preserve the stratigraphic

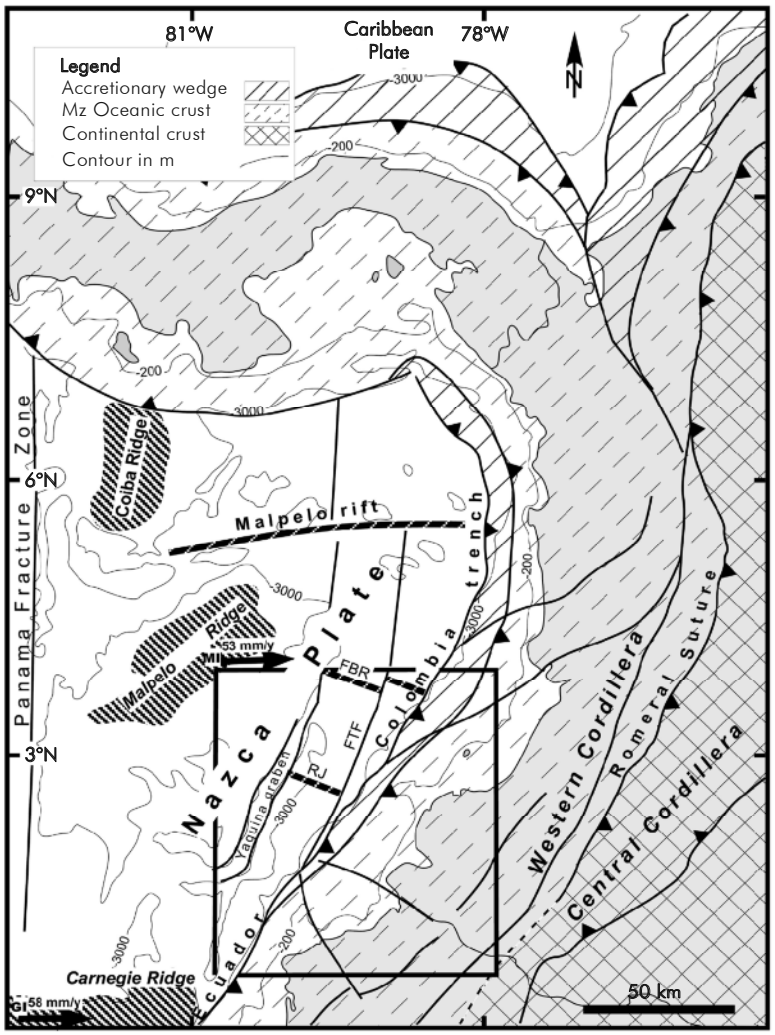

Figure 1. Regional tectonic map with the distribution of major blocks and faults along the Northwestern South American Margin (Modified from Mountney and Westbrook, 1996; Cediel et al. 2003). Note the distribution of Mesozoic oceanic crust, bounded to the East by pre-Mesozoic Continental crust along the Romeral Suture and to the West by the Nazca Plate (Ecuador – Colombia trench). Along the trench the continental sediments form the accretionary wedge. Observe the progressive decrease in the sedimentary accretionary wedge width along the Northern Ecuadorean to Southern Colombian (NESC) margin (cross-hatched area, bounded by thick black line), reflecting the transition from tectonic accretion in the north to a tectonic erosion regime in the south. The Nazca Plate shows numerous structures including ridges (Malpelo, Carnegie and Coiba ridges), Rift Jump (RJ), Fossil Buenaventura Rift (FBR), and Malpelo Rift (MR), Fossil Transform Fault (FTF) and Panamá Fracture Zone), which derive from the complex geologic evolution of the region (Modified from Hardy, 1991). Convergence rates at Galapagos Island (GI) and Malpelo Island (MI) from Trenkamp et al. 2002). The region outlined by thick dark line shows the area of interest for this study.

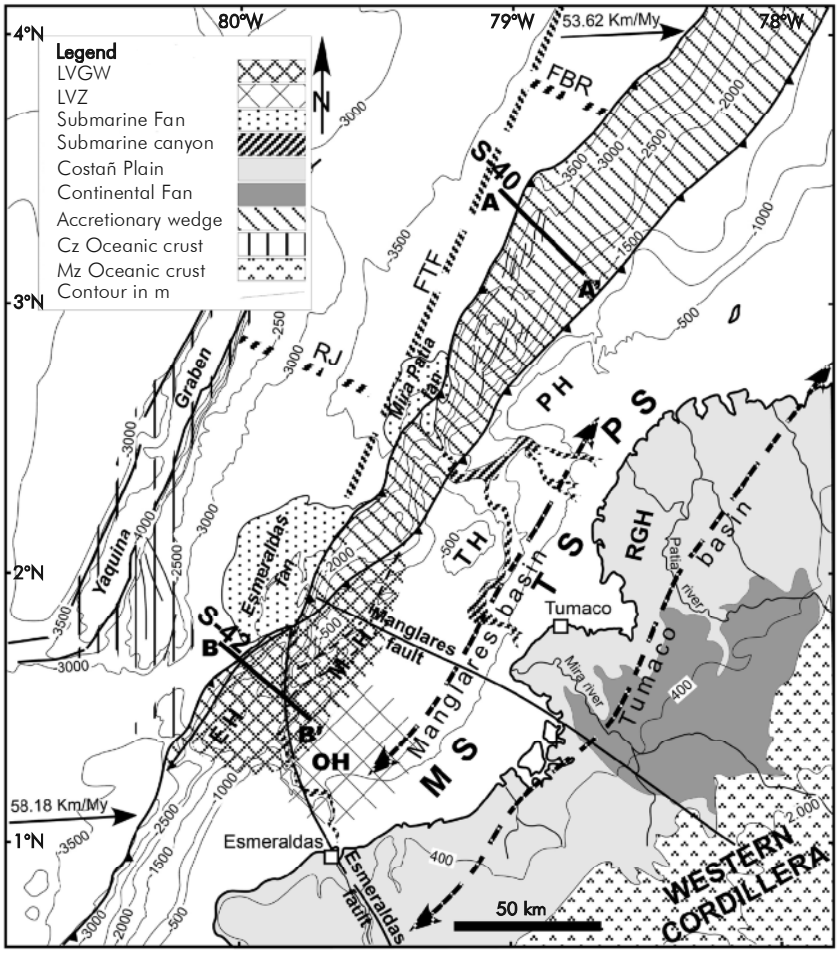

Figure 2. Map with the main morphologic and tectonic features observed along the NESC. The margin is bisected by several submarine canyons (Esmeraldas, Mira and Patia), that provide sediments to associated, distal submarine fans. The Tumaco and Manglares basins are oriented parallel to the subduction zone, divided by the Remolino Grande High (RGH), outlining a double forearc basin system. A discontinuous chain of structural highs known as Esmeraldas (EH), Manglares (MH), Tumaco (TH) and Patia (PH) outline the seaward border of the NESC margin double forearc basin. To the west of these structural highs the accretionary wedge increases in width toward the North, suggesting a transition from tectonic erosion in the south to a regime of tectonic accretion in the north (modified from Marcaillou et al. 2006 and Marcaillou et al. 2008). Note that the overriding plate is segmented by the Manglares and Esmeraldas faults that divide the thermal structure of the NESC margin into the Manglares (MS), Tumaco (TS) and Patía (PS) segments (modified from Marcaillou et al. 2008). In the Manglares segment seismic refraction experiments have detected altered basement zones known as the Low Velocity Zone (LVZ) and Low Velocity Gradient Wedge (LVGW) (modified from García – Cano et al. 2014 and Collot et al. 2008). To the west of the Manglares segment, the basement of the Nazca Plate is extensively exposed at the sea floor along the Yaquina Graben walls. In addition, seamounts are faulted by the Fossil Transform Fault (FTF) and Ridge Jump (RJ) structures. (Hardy, 1991). Heavy lines (S-40 and S-42) indicate lines of cross sections shown in the Figure 3.

record of the margin deformation during the Cenozoic (Marcaillou and Collot, 2008). The bathymetric, seismic and gravimetric data reveal that these basins are divided by elongated basement highs parallel to the subduction zone (the Esmeraldas, Manglares, Tumaco, Patía and Remolino Grande highs), forming a double forearc basin system (Figure 2). Based upon analysis of seismic data, seismological information and heat flow measurements, the double forearc basin system is affected by a system of cross-sectional structures that segment the NESC margin into the Manglares, Tumaco, and Patía segments (Collot *et al*. 2004; Marcaillou *et al*. 2008, Marcaillou *et al*. 2006 a).

In accordance with the field geology studies (Gansser, 1950; Echeverria, 1980; Evans and Whittaker, 1982), and high quality seismic reflection profiles (Marcaillou and Collot, 2008; Collot *et al*. 2008), the basement into the NESC margin is strongly structured and controls the distribution and thickness of the pre-Oligocene sedimentary units. The paleomagnetic and tectonic data suggest that the Northwestern South

American convergent margin was experiencing a transpressive tectonic regime during the Paleogene (Daly, 1989; Luzieux *et al*. 2006) and a subsequent compressive regime during the Neogene (Marcaillou and Collot, 2008). These changes in the tectonic regime during the Cenozoic (transpressive to compressive) along the convergent margin occur as the direction and convergence rates between the South America and Farallon plates changed (Pardo – Casas and Molnar, 1989), and coincide with the fragmentation of the Nazca – Cocos plates (Lonsdale and Klitgord, 1978). In this context, the Nazca Plate is a remnant of the Farallon plate dating from late Oligocene to middle Miocene. (Lonsdale, 2005; Lonsdale and Klitgord, 1978). The time at which the Nazca Plate began subducting beneath the Northwest South American Plate remains unknown. Paleogeographic reconstructions suggest that the convergence rate between the two plates has been variable during the Neogene (Pardo – Casas and Molnar, 1987), suggesting that the period following the break-up of the Farallon Plate was followed by the development of numerous ridges, rifts, grabens and transform faults (Figure 1). The activity that formed these features ended during the middle Miocene (Hardy, 1991; Meschede and Barckhausen, 2000). Some fossil rift and transform structures near the trench have been filled with sediments carried by the Patía – Mira and Esmeraldas submarine canyons systems (Figure 2). At the toe of these canyons systems, bathymetric data and seismic reflection profiles reveal the development of several submarine fans (Figure 2), some of them over 200 km wide, 575 km long and containing a sediment column from 2 to 4 km thick. The sediments within these fans will eventually be subducted along the NESC margin (Marcaillou *et al*., 2008). These submarine fans are fed by canyons from the continent by the Patía, Mira and Esmeraldas catchment basins, which originate along the upper slopes of the Western Cordillera (Figure 2). The Esmeraldas submarine fan is more than 4 km thick along its axis (Figure 3), while the Mira – Patía submarine fan is less than 2 km thick (Marcaillou *et al*. 2008). Piston core samples recovered during the AMADEUS cruise (Collot *et al*. 2005 a), showed that the submarine fans of the NESC are primarily composed of thick sequences of muds and clays, interbedded with fine to very coarse grain sandstones, beds of volcanic ash, and centimeter scale fragments of wood and plants. Samples recovered by dredges from the proximal areas of the Esmeraldas and Mira – Patía submarine fans show well rounded sediments with sizes ranging from cobbles to pebbles that suggests the occurrence of high energy transport events feeding sediment to the trench (Collot *et al*. 2005 a).

Pre-stack depth migration of multichannel seismic lines (PSDM) across the Tumaco and Patía segments (Marcaillou *et al*., 2008) show that a great portion of the sediments transported to the trench have been accreted along the margin, forming an accretionary wedge over 30 km wide cut by numerous thrust faults (Figure 3a). Samples recovered by dredges from the lower and middle parts of the continental slope of the Tumaco and Patía segments, show that sediments involved in the accretionary wedge are similar to the sediments recovered by piston cores in the submarine fans. However, the sediments included in the accretionary wedge are more compacted and foliated than sediments recovered from the submarine fans (Collot *et al*. 2005 a). In the southern portion of the study area, a PSDM seismic line across the Manglares segment (Collot *et al*., 2008) shows that a small portion of the sediments of the Esmeraldas submarine fan have been accreted along the margin forming a sedimentary accretionary wedge of less than 5 km wide (Figure 3b). Finally, across the Esmeraldas high interpretation of the seismic lines shows that the slope margin was affected by normal faulting, while a significant accumulation of sediments (>2 km) were deposited in the subduction trench during the Pleistocene to Holocene (Figure 3), including submarine slides originating from the overriding plate (Collot *et al*. 2008; Sage *et al*. 2006, Calahorrano *et al*. 2008). These variations along the NESC margin probably reflect a change in the type of subduction between tectonic accretion (Tumaco and Patía segments) and tectonic erosion (Manglares and Esmeraldas segments) (Marcaillou, 2003).

The change in the type of subduction along the NESC margin from accretion to erosion coincides with lateral variations in the interplate contact and the thermal structure. A detailed geophysical study toward the south of the Manglares segment (undergoing tectonic erosion), shows graben structures in the upper part of subduction trench, fully covered by sediments (up to 2 km thick) with highly over-pressured fluids that decrease the amount of coupling between the upper and lower plate (Sage *et al*. 2006). In the Manglares segment (also undergoing tectonic erosion), the presence of crustal faults connected with the subduction trench (Figure 3b)

favors the escape of fluids to the surface, contributes to the alteration of the overriding plate, and increases the conditions of interplate coupling (Collot *et al*., 2008). In the Tumaco and Patía segments (undergoing tectonic accretion), a study of the bottom simulating reflector (BSR) and heat flow measurements suggest that fluids produced along the top of the subducting plate migrate up to the sea floor via thrust faults within the accretionary wedge (Collot *et al*. 2005). Additionally, variations in the thickness of sediments being subducted below the NESC margin have been proposed as the cause of the segmentation of the thermal structure across the Manglares, Tumaco and Patía segments, based upon regional analysis of the BSR and heat flow measurements (Marcaillou *et al*. 2008) (Figure 2).

Based upon 3D seismic refraction data in the NESC margin, a sub-horizontal Low-Velocity Zone (LVZ) ES defined (Figures 2, 3b), within the basement of the overriding plate along the Manglares segment, at depths between 5 to 15 km. The LVZ is ~40 km wide, 50 km long, and more of 5 km thick, with P-wave velocities values of 350 m/s lower than the velocities of the overlying rocks (Garcia – Cano *et al*. 2014). This LVZ is bounded at the top by a highly reflective interval named unit G, strongly affected by faults (Collot *et al*, 2008), and its base is defined by the basal detachment (Figures 2 and 3b). Laterally, the LVZ is bounded by faults and structural highs that involve uplifted basement rocks along the splay fault beneath the Ostiones high and by the Manglares high to the west (Figure 2). (Garcia-Cano *et al*., 2015; Marcaillou et.al., 2008). The presence of similar LVZs has been proposed in other subduction zones along the Northern Pacific coast of Chile, Costa Rica and Cascadia, having diverse mechanisms to explain their origin. In the Northern Chilean subduction zone (undergoing tectonic erosion), the presence of a LVZ has been construed as the result of a gradual accumulation of fluids below a structural detachment in the overriding plate that were expelled from sediments involved in subduction (Sallarès and Ranero, 2005). In the Costa Rican subduction zone (also undergoing tectonic erosion), a LVZ is interpreted as the result of the alteration of highly deformed and fractured basement rocks into the upper plate, altered by fluids expelled from the sediments along the basal detachment (Christeson *et al*. 1999). In the Cascadian subduction zone (undergoing tectonic accretion), a LVZ has been interpreted as a result of a combination of alteration of peridotitic rocks to serpentinitic rocks and underthursting in the overriding plate (Hyndman and Peacock, 2003). In accordance with the field geology studies (Gansser, 1950; Echeverria, 1980; Evans and Whittaker, 1982), and high quality seismic reflection profiles (Marcaillou and Collot, 2008; Collot *et al*. 2008), the basement into the NESC margin is strongly structured and controls the distribution and thickness of the pre-Oligocene sedimentary units. The paleomagnetic and tectonic data suggest that the Northwestern South American convergent margin was experiencing a transpressive tectonic regime during the Paleogene (Daly, 1989; Luzieux *et al*. 2006) and a subsequent compressive regime during the Neogene (Marcaillou and Collot, 2008). These changes in the tectonic regime during the Cenozoic (transpressive to compressive) along the convergent margin occur at the same time that the direction and convergence rates between the South America and Farallon plates changed (Pardo – Casas and Molnar, 1989), and coincides with the fragmentation of the Nazca – Cocos plates (Lonsdale and Klitgord, 1978). This tectonic evolution suggests that the origin of the LVZ in the Manglares segment is associated with the high structuration of the overriding plate, the change in the tectonic regime experienced along the NESC margin during the Cenozoic and the evolution of the subducting plate.

The NESC margin was ruptured in 1906 by a single thrust event of Mw 8.8 (Kelleher, 1972; Kanamory and McNally, 1982). Several minor events were reported along the NESC margin and have made it possible to propose a recurrence interval of 70 years for the area (Beck and Ruff, 1984). In areas with compressional tectonic settings, the numerical modeling shows that huge volumes of fluids are primarily expelled during the interseismic and over-compressed stages while during the coseismic stage the fractures are opened, causing the decrease of fluid pressures and the migration of new fluids into the hanging wall block (Doglioni *et al*. 2013).

During the last decade, a number of scientific cruises and hydrocarbon exploration missions along the NESC margin have provided rock and sediment samples with thermogenic oil and gas traces (Collot *et al*. 2005a; ANH, 2014). A few samples of calcareous crust fragments rich in shells of bivalves (Figure 4), obtained from the middle to the lower part of the accretionary wedge (Collot *et al*. 2005a), show isotopic signals in ∂13C indicative of a thermogenic fluids source (López, 2009). Six piston core

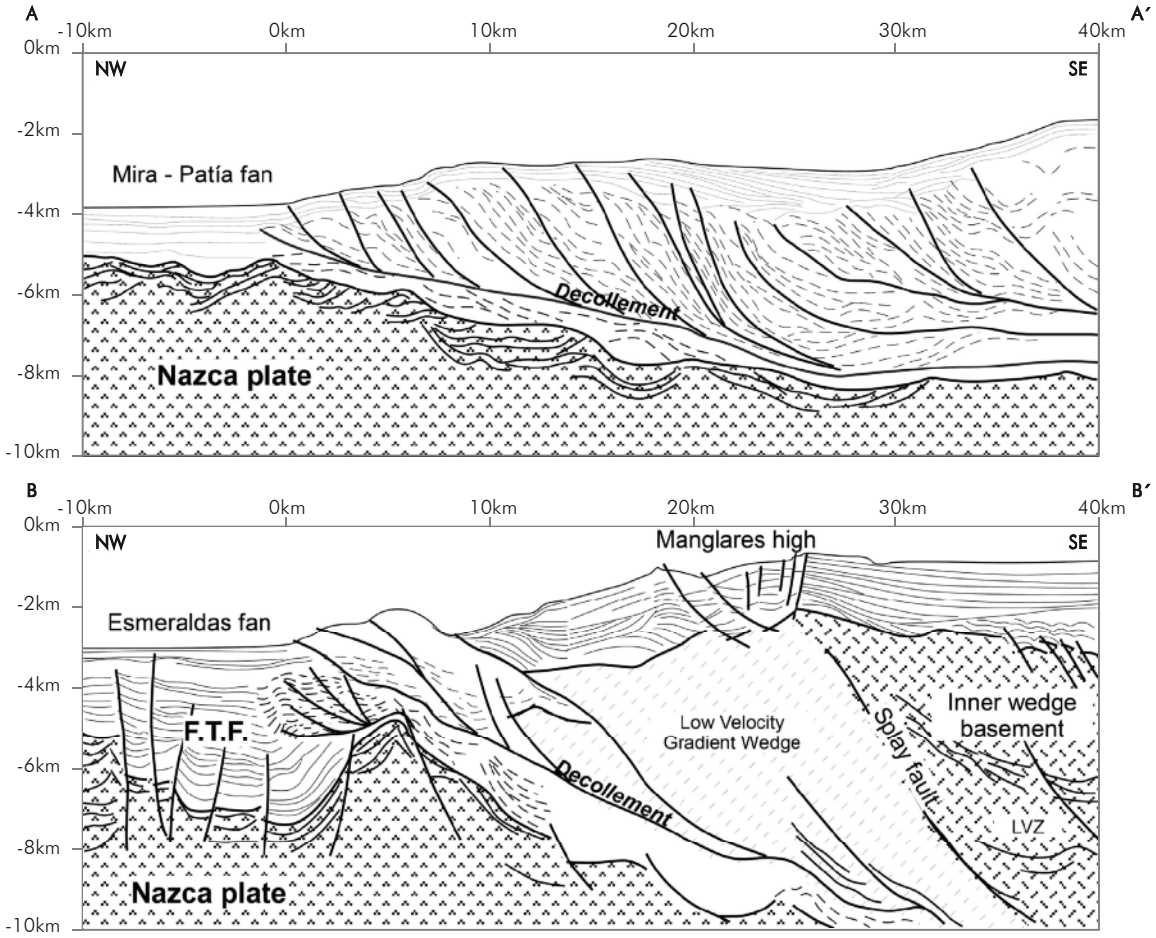

Figure 3. Cross-sections derived from pre-stack depth migrated seismic reflection data that illustrate the structural and morphological changes that occur along the middle and lower continental slope of the NESC margin (location shown in Figure 2). The northern cross-section (top, line A to A') (Marcaillou et al. 2008) shows a broad accretionary wedge involving up to 2km of sediments and include the Mira – Patía submarine fan. The southern cross-section (bottom, line B to B'), in comparison, illustrates a much narrower accretionary wedge. Note the thick package of the sediments associated with the Esmeraldas submarine fan entering the subduction zone along with fragments of the overriding plate and the development of a LVGW (Collot et al. 2008). In addition, the structural expression along the top of the underlying Nazca Plate changes from North to South with little faulting in the North (top) while in the South (bottom) the basement is strongly faulted (proximal to the trace of the FTF) and evidence of seamounts (SM).

samples (average 1 m thick) were recovered in 2009 by the Colombian state oil company ECOPETROL along the seaward border of the NESC's outer highs (Figure 4). Geochemical analysis of head space and occluded gases from the middle and bottom part of each piston core, indicate levels of C1 between 5 to 100 ppm, traces of C2 to C4 between 0.1 to 1 ppm, and levels of i-C5 and n-C5 between 1 to 100 ppm (Figure 5). Additionally, quantitative diamandoid analysis in the same samples shows concentrations of 3- + 4- methyldiamantenes and 1- + 2-methyladamantanes that support the existence of traces of thermogenic hydrocarbons in the area (Figure 6). The concentrations of diamandoids suggest an increase in the presence of thermogenic oils, from southwest to northeast, parallel to the strike of the NESC slope (Figure 4). These geochemical indications provide constraints for our 2D TTIArr modeling as described below.

3. DATA AND METHODOLOGY

In order to explain the origin and distribution of the thermogenic hydrocarbons reported along the accretionary wedge and outer backstop basement of the NESC margin, a series of 2D numerical models were constructed to show the variation of the *TTIArr* along the subduction zone. Lateral changes along the NESC margin including the degree of tectonic erosion (Collot *et al.* 2008), the width of the accretionary wedge, the thickness of sediments, and variations of the thermal structure (Marcaillou *et al.* 2008; López, 2009) were

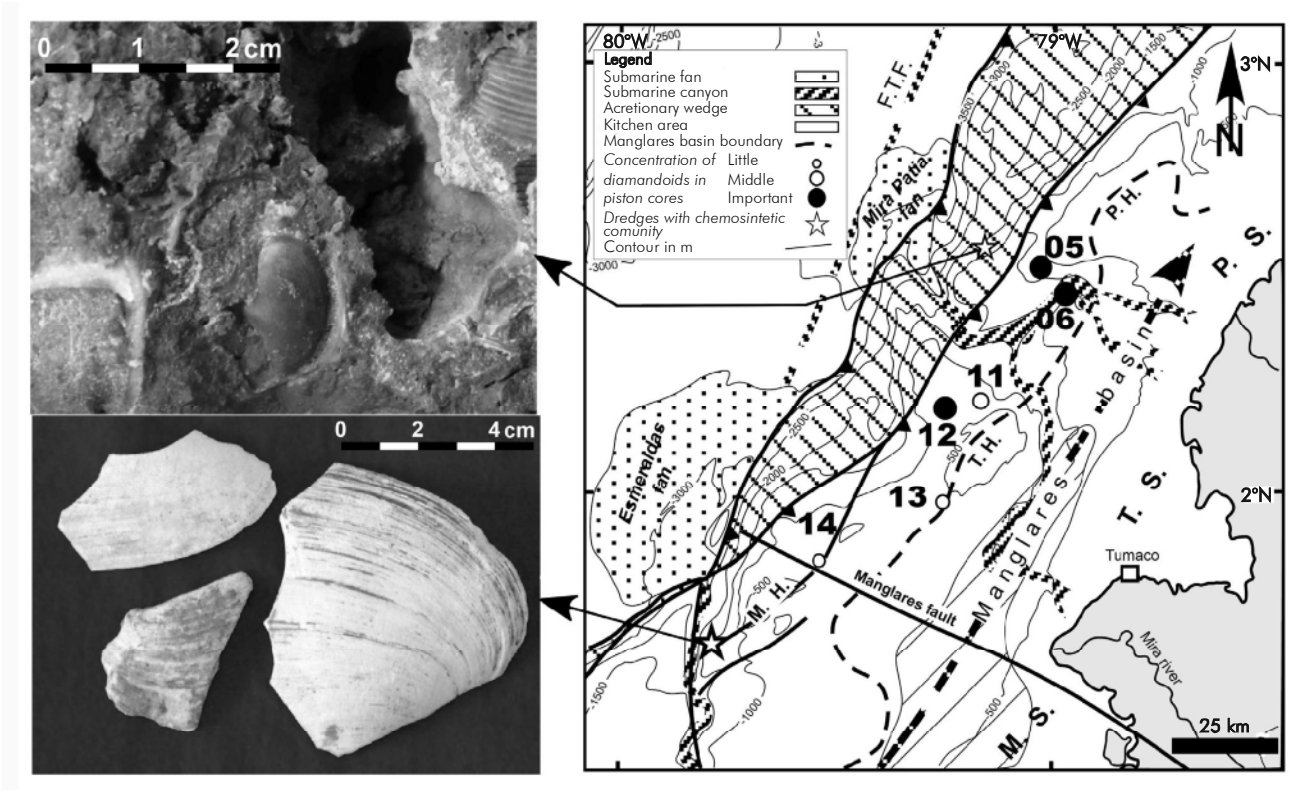

Figure 4. Location map of samples recovered from the seafloor with evidence of thermogenic fluids along the lower and middle slope of the NESC margin (right). Note that the samples are located 30 to 60 km to the west of the potential hydrocarbon generation kitchens located within the Manglares basin (bold numbers show the piston core locations). Small white circles indicate the location of piston core samples with trace evidence of thermogenic hydrocarbons (*<10 ppm*), medium sized white circles show the location of piston core samples with fair indications of thermogenic hydrocarbons (10 – 30 ppm) and large black dots represent the location of samples recovered with strong indications of thermogenic hydrocarbons (>30 ppm)) White stars show the location of samples recovered by dredges during the AMADEUS cruise (Collot et al. 2005), with fragments of calcareous crust rich in bivalve shells interpreted as chemosynthetic communities (left). The calcareous crust fragments close to the Manglares high (M. H.), show isotopic signals in ∂13C indicative of a thermogenic fluids sourced from the subduction zone.

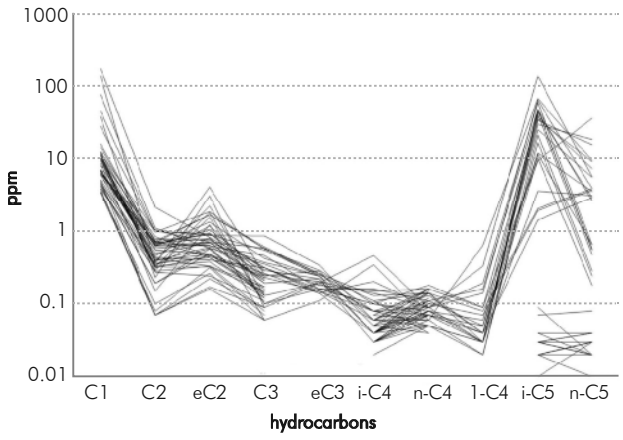

Figure 5. Graphic of concentrations in ppm of all the hydrocarbons analyzed presented in the headspace and adsorbed gas samples recovered at the base, middle part and top of each piston core in the slope zone of the NESC margin. Note the increase in the concentration of i-C5 in all samples. Methane (C1), Ethane (C2), Ethene (eC2), Propane (C3), Propene (eC3), iso butane (i-C4), normal butane (n-C4), 1-butene (1-C4), iso pentane (i-C5) and normal Pentane (n-C5).

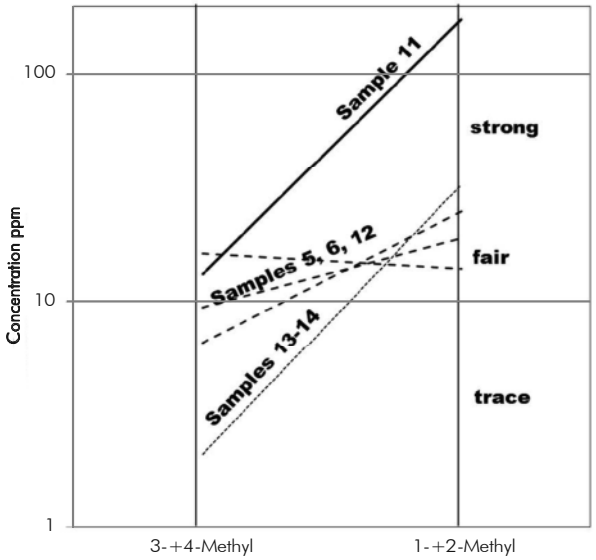

Figure 6. Graphic of concentration in ppm of 3- + 4- methyldiamantenes and 1- + 2-methyladamantanes. Note that the samples recovered to the south of the Tumaco high show less concentrations in diamandoids in comparison with the samples analyzed to the North.

incorporated into 5 regional cross sections, upon which the *TTIArr* modelling is based (Figure 7). The results of the 2D *TTIArr* models along the various cross sections were compared in order to identify variations in the depth and width of the oil and gas generation windows along the top of the subducting plate (Figure 7).

To further constrain numerical models along the subduction zone, additional data were incorporated including the structural history of the NESC margin during the Quaternary (López, 2009), the thermal structure along each section, and the selection of the kinetic parameters for the organic matter included in the subduction, taking into account the type of kerogens reported in the NESC margin by exploratory wells (*ANH, 2014*). The 5 regional sections are ~270 km long each and oriented perpendicular to the margin, (Figure 7). The first regional cross sections is located through the Patía segment (Section 1), the second section is located across the Tumaco segment (Section 2), the third section is located at the boundary between the Tumaco and Manglares segments (Section 3) and the final two sections are located within the Manglares segment (Sections 4 and 5). In each of these sections, the

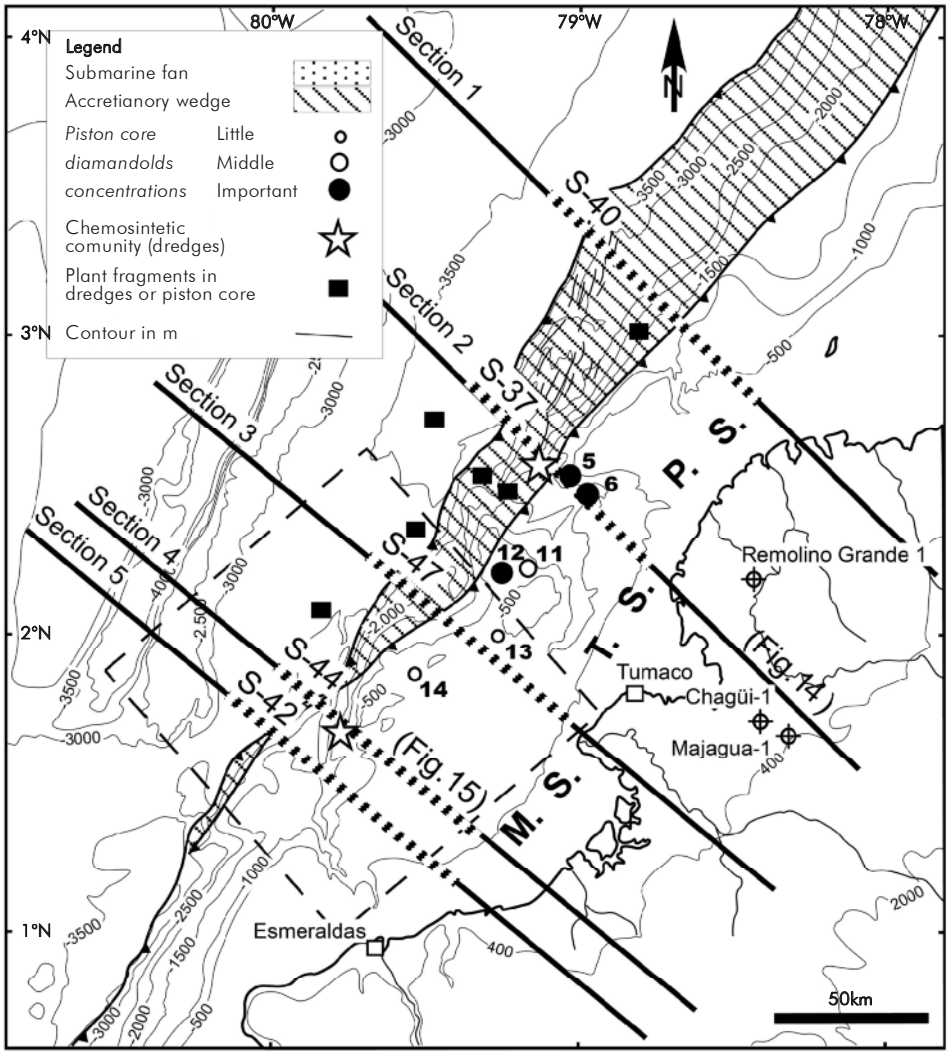

Figure 7. Location of regional cross sections (lines 1-5) used to construct 2D *TTIArr* models along the NESC margin subduction zone. Line segments with diagonal white pattern indicate the location of multichannel seismic reflection profiles (S-37, S-40, S-42, S-44 and S-47) used during the construction of the structural geometry of each section (modified from Marcaillou et al. 2008; Collot et al. 2009). TOC values in the Tumaco basin was obtained from the exploratory wells drilled in the Tumaco basin described by Cediel et.al (2009). Black squares show the location of the piston cores and dredges with fragments of plants carried from the forearc zone (Collot el.al., 2005). The dashed line box shows the location of the ESMERALDAS 3D seismic refraction survey (modified from García – Cano et al. 2014). Piston core (circles) and dredges samples (white stars) are the same described in the Figure 4. The Manglares (MS), Tumaco (TS) and Patía (PS) thermal segments correspond to the definition of Marcaillou et al. (2008).

western end (~100 km) extends onto the oceanic plate, and the eastern part (~170 km) covers the overriding plate, including the accretionary wedge, forearc basin and volcanic arc (Figure 7). Bathymetric chart information were used to build the margin morphology along each regional cross section (Collot *et al*. 2009; Collot *et al*. 2005 a). Based upon this information, the subduction trench axis is located ~3.6 km below sea level, approximately ~90 km to the west of the present-day coast line, with sea floor slopes along the lower and middle slope between 3° and 6°, and slopes along the upper slope and shelf zones of 1° or less (Table 1).

Wide angle seismic information provides crucial data to constrain the crustal structure of the NESC margin. This data includes the crustal thickness of the Nazca and South American plates, the distance from the backstop basement to the trench axis, the variations in the dip of the top of the subducting plate along the westernmost 60 km of the subduction zone, the depth of the mantle wedge (portion of the mantle bounded by the top of the subducting plate and the base of the overriding plate) and the thickness of the sediments being subducted (Table 1). The seismic refraction data indicates that the Nazca Plate is ~ 6 km thick (Marcaillou *et al.* 2006 b; Agudelo *et al*. 2009), while the South American Plate is ~30 km thick (Meissnar *et al*. 1976; Case *et al*. 1973). The available gravimetric and seismic refraction data suggest that the distance between the backstop basement boundary and the trench axis varies from ~10 km in the Manglares segment (Agudelo *et al*. 2009) to 30 km in the Patía segment (Mountney and Westbrook, 1996; Marcaillou *et al*. 2008). Velocity models in the Manglares segment point to the existence of an outer basement block with a low velocity gradient along the seaward backstop border (Collot *et al*. 2008).

The structural model of the subduction zone along the NESC margin is one of the most important elements required to properly constrain the *TTIArr* modelling. The structural model incorporates variations of the dip of the top of the subducting slab as a function of the depth along each regional cross section. In the upper part of the subduction zone (between 0-10 km of depth), the dip of the top of the subducting plate increases from 9° to 11° (Marcaillou *et al.* 2008.; Agudelo *et al*. 2009), between 10-30 km, the dip of the subduction plane increases to between 15° to 17° (Agudelo, 2005; Garcia – Cano *et al*. 2014; Agudelo *et al*. 2009). In the deeper part of the subduction zone (from 30-60 km), the top of the subducting plate dips to the east at ~23° (Trenkamp *et al*. 2002; Manchuel *et al*. 2011) (Table 1).

Table 1. Synthesis of values used to build the morphology (according to Collot et al. 2005 a) and crustal geometry of the five sections (S1 to S5) along the NESC margin (after Agudelo et al. 2009; Collot et al. 2008; Agudelo, 2005; Trenkamp et al. 2002; Marcaillou et al. 2006; Marcaillou et al. 2008; Meyer et al. 1977; Meissnar et al. 1976).

MARGIN MORPHOLOGY						
Element		**Section 1**	**Section 2**	**Section 3**	**Section 4**	**Section 5**
Trench Depth (KM)		4	3.6	3.5	3.2	3.5
Trench - Coast Line Wide (KM)		90	80	80	100	100
Lower Slope Dip		3°30´	3°30´	2°45´	6°30´	6°30´
Upper Slope + Shelf Dip		1°	1°	1°	<1°	<1°
CRUSTAL MARGIN GEOMETRY						
Nazca Plate Thickness				6 km		
South American Plate Thickness				30 km		
Back Stop Boundary		30	15	5	10	10
Subduction Plane Dip	0 - 10 km	9°	10°	9°	9°	9°
	10 - 30 km	15°	16°	15°	15°	15°
	> 30 km			23°		
Thickness of Sediment in Subduction (Km)		1.2	3.5	4.5	3	3
Wide and Depth of the LVZ			No recorded		15 km (wide), 7 km (depth)	

The thickness of the sediments undergoing subduction below the lower and middle slope areas of the NESC margin varies from 2 to 4 km, according to seismic reflection and refraction profiles (Marcaillou *et al*. 2008) (Table 1). The structural model of the NESC margin is further refined using the results of 3D seismic refraction experiments showing a 15 km wide LVZ, at 7 km below sea floor, in the basement of the Manglares segment with a velocity gradient of 0.13 km/s/km (Garcia-Cano et.al,, 2015). The convergence rates measured between the Nazca and South America plates have been used to define the subsidence rate of the sediments along the top of the subducting plate. The present convergence rates (Figure 1) vary from 58 mm/y near The Equator to 53 mm/y at 4°N (Trenkamp *et al*., 2002). These values have been interpolated at each cross section along the NESC margin and adjusted for the difference in angle between the convergence vector and the strike of each section resulting in calculated convergence rates of ~39 mm/y along sections 1 and 2 and rates of ~40 mm/y along sections 3 to 5.

The thermal structure of the NESC margin is another basic component required to constrain the *TTIArr* models along the subduction zone. Using available information including detailed studies of the BSR, heat flow measurements, and finite element models (Marcaillou *et al*. 2006 a; Marcaillou *et al*. 2008), functions of temperature vs. depth were constructed along the subduction zone in four of the five regional cross sections. The thermal structure of section 5 was used in the 4th section, because of the close proximity of the two sections.

Based upon the structural history, thermal structure, and kinetic parameters of the organic matter in the NESC margin, we made a series of 1D *TTIArr* model at one kilometer intervals along each of the five sections to identify the conditions of hydrocarbon generation in the sediments along the top of the subducting plate. The 1D *TTI* based on the Arrhenius equation was derived by Wood (1988) and expressed as:

$$TTIArr = \frac{A(t_{n+1}-t_n)}{T_{n+1}-T_n}\left\{\left[\frac{RT^2_{n+1}}{E+2RT_{n+1}}Exp\left(\frac{-E}{RT_{n+1}}\right)\right] - \left[\frac{RT^2_{n}}{E+2RT_{n}}Exp\left(\frac{-E}{RT_{n}}\right)\right]\right\} * 100 \quad (1)$$

where *tn* and *tn+1* are, respectively, the time (Millons of Years) AT absolute temperatures *Tn* and *Tn+1* (°C + 273) occurred. *R, E* and *A* correspond with the kinetic parameters expressed in the Arrhenius equation, where *R* is the ideal gas constant, *E* is the energy activation in kj/mol and *A* is the factor of frequency (1/m.y.). Standard values of kinetic parameters (*R, E* and *A*) were selected based upon the type of organic matter documented in the NESC (type II to type III kerogen) (Cediel *et al*. 2010). According to Hunt *et al* (1991) and Hunt and Hennet (1992) type II - III kerogens have slow to medium rates of reaction, activation energy values (E) between 218 to 230 kj/mol, frequency factors (A) from $5.656*10^{26}$ to $3.98*10^{27}$ 1/my and propensity to generate gas (Hunt and Hennet, 1991).

Over time, the organic matter maturation is additive and the total maturity of the sediments is given by the sum of the maturity reached at each interval, expressed as:

$$TTIArr_{(total)} = \sum_{nmin}^{nmax} TTIArr_n \quad (2)$$

Where nmin and nmax correspond to the minimum and maximum temperature values of the calculated intervals. The values of *TTIArr* obtained along each section allow for defining the windows of oil and gas generation and preservation (Table 2) according to the threshold values defined by Lopatin (after Waples, 1980). Additionally, the values obtained for *TTIArr* allow us to calculate the percentage of expelled oil (X%), using the following expression developed by Hunt *et al*. (1991):

$$X\% = [1-\exp(-TTIArr(total)/100)]*100 \quad (3)$$

Table 2. Threshold values of Lopatin's time – temperature index of maturity (TTI) and hydrocarbon zones (modified from Waples, 1980). Values in parentheses correspond to oil generated percentages based on Hunt et al. (1991).

Lopatin Threshold Value (TTIArr)	Hdrocarbon Zone (% Oil Generated)
15 - 75	Begin oil generation (0 - 50%)
75 - 160	End oil generation (50% - 80%)
160 -~500	Oil preservation <40°C (80% -)~100%)
~500-~1000	Oil preservation <50°C
~1000-~1500	Wet gas preservation
~1500 - 65000	Dry gas preservation

The result of each 1D model was plotted along each section, in order to show the zones of generation of oil and gas along the top of the subducting plate. In addition, the location of samples with traces of gas or condensate of thermogenic origin (Figure 4) are projected onto each section to establish possible migration pathways from the sediments along the top of the subducting plate to sea floor.

Model assumptions

To carry out the construction of the 2D TTIArr models along the top of the subducting plate, it was necessary to assume that the crustal geometry, convergence rates, and thermal structure in each one of the sections has been constant during the last 3 m.y. This is the minimum time required to carry the subducting sediments from the trench to the mantle wedge based upon the convergence rates between the Nazca and South American plates has averaged ~60 km/m.y. during the last 10 m.y. (Pardo – Casas and Molnar, 1987; Kendrick *et al*. 2003) and the Nazca Plate expansion activity ended at 5 m.y. (Lonsdale and Klitgord, 1978; Hardy, 1991). Under these conditions it is possible to consider that the crust of the NESC margin has similar geometry and dynamics during the last 3 m.y.

To model the organic matter content in the sediments involved in the subduction zone, it was assumed that the sediments in the trench contain organic matter (kerogen type IID) reworked from the continent, similar to the sediments and rock samples recovered in the submarine fans close to the trench (Esmeraldas and Mira – Patía). These samples contain abundant fragments of wood and dark intervals with organic matter, sourced from the land and near-shore zones. Similar conditions of high energy and high sedimentation rates in convergent margins are considered by Littke and Sachsenhofer (1994) as the main mechanism of transport and preservation of organic matter in sediments involved in subduction.

The *TTIArr* modelling is focused on the upper part of the sediments parallel to the basal detachment (décollement) and assumes a uniform thickness and isotropic distribution of organic matter within the sediments without thickness changes associated with the compaction or expulsion of fluids from the mantle wedge. The modelling is restricted to sediments along the décollement plane based upon several wells that have penetrated subduction zones in other convergent margins around the world that shows evidence of fluids and gas (water and hydrocarbons) of thermogenic origin very close to the top of the sediments involved in subduction or at the base of the accretionary wedge (Behrmann *et al*. 1992; Kimura *et al*. 1997; Taira *et al*. 1991; von Huene *et al*. 1977). As stated by Tobin *et al* (2001), the upper part of the sediments involved in subduction acts as effective lateral migration pathway of fluids and gas of thermogenic origin, while the middle and lower part of the sediments act as a seal for vertical migration of fluids.

3. RESULTS AND DISCUSSION

Thermal structure and distribution of zones of oil and gas generation and preservation along the NESC margin

The results of the 2D *TTIArr* models are presented along the cross sections, integrating the available geophysical information and surface locations with evidence of oil and gas seeps. These cross sections allow for the identification of possible migration pathways and areas of entrapment for hydrocarbons generated along the subduction zone. The 2D *TTIArr* modeling along the NESC margin show that the sediments transported by the Nazca Plate and subducted below the South American Plate are now experiencing favorable conditions for generation of thermogenic oil and gas (Figures 8 to 12). Along cross sections 1 to 3 (Figure 7), the *TTIArr* modelling indicates that the generation and preservation of oil and gas in the sediments along the top of the subducting plate occurs in a ~30 to 40 km wide zone. The generation and preservation of oil occur in the westernmost ~10 km (where 80 to 100% of oil expulsion occurs), and the generation and preservation of wet and dry gas occur in deeper areas that lie along the eastern ~25 km of the zone (Figures 8 to 10). The modelling in the Patía and Tumaco segments suggests that the depth of the oil generation zone along the decollement begins at 11 km along section 1 to the north and increases up to 14 km toward section 3 to the south. The top of the oil preservation zone is present along section 1 at ~14 km and increases to ~16 km along section 3 (Figures 8 to 10). Below the oil preservation zones, the generation of wet and dry gas occurs at depths below 18 km in the Patía segment (section 1) and below 24 km in the Tumaco segment (section 3) prior to contact with the overriding plate moho (Figures 8 to 10). In addition, the models indicate that the distance between the trench axis and the beginning of the oil generation zone increases from north to south, from ~45 km to ~ 55 km (Figures 8 to 10).

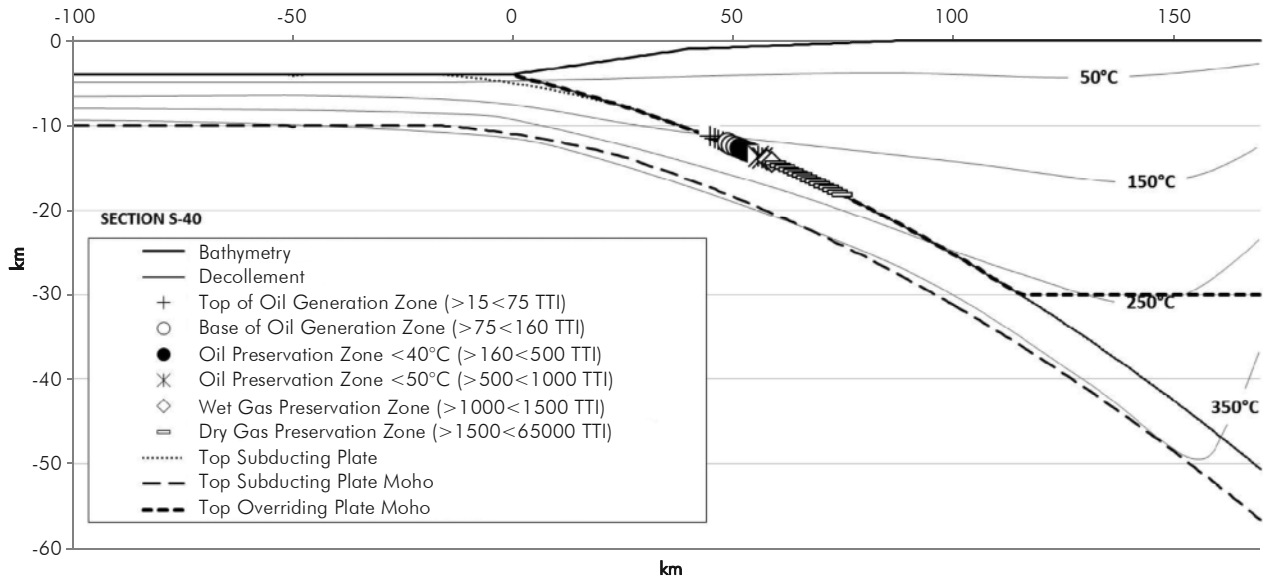

Figure 8. Present day hydrocarbon generation zones (oil and gas) as predicted by the 2D *TTIArr* modeling along the subduction zone in section 1 (see location in the Figure 7). This section represents the structure of the margin in the Patía segment. Vertical exaggeration = x 2.

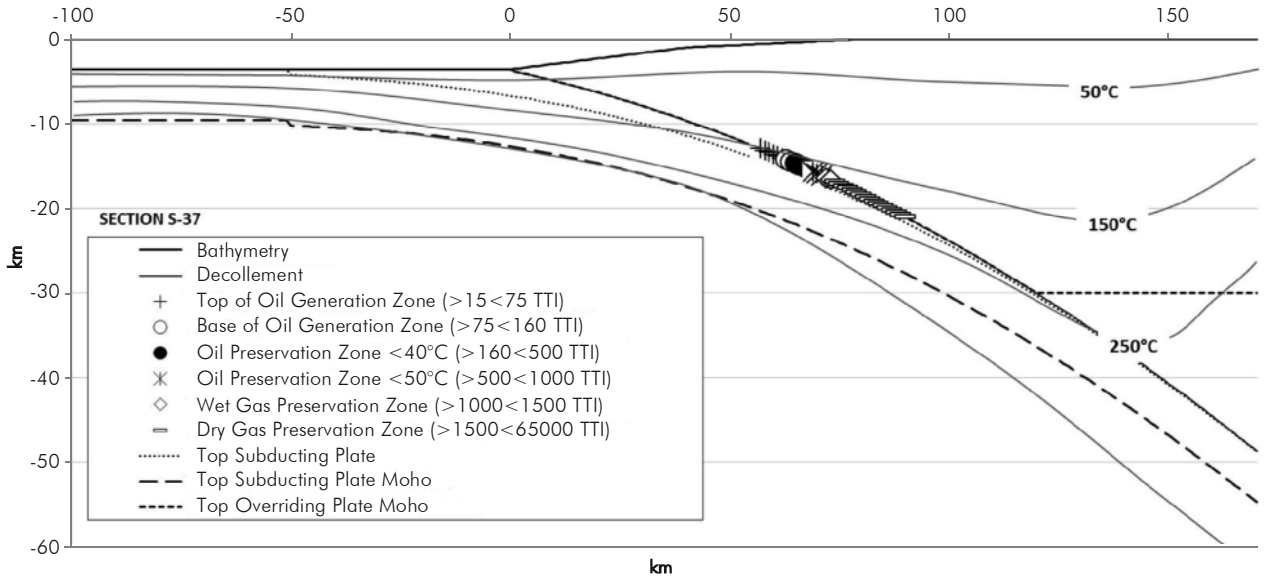

Figure 9. Present day hydrocarbon generation zones (oil and gas) as predicted by the 2D *TTIArr* modeling along the subduction zone in the section 2 (see location in the Figure 7). This section represents the structure of the margin in the Tumaco segment. Vertical exaggeration = x 2.

In the Manglares segment (Figure 7), the models along sections 4 and 5 indicate that the conditions of generation and preservation of oil and gas occur in a ~45 km wide zone along the top of the subducting plate. The generation and preservation oil occurs in the westernmost 20 km of the zone and the generation and preservation of wet and dry gas occurs in the remaining 25 km to the east (Figures 11 and 12). The beginning of the oil generation zone occurs at a depth of 16 km, located ~60 km to east of the trench axis. At depths of ~20 km 80% of the oil is expelled and at depths of 22 km 100% of the oil is expelled (Figures 11 and 12). Below this depth, the models show favorable conditions for generation of wet and dry gas prior to the sediments coming into contact with the mantle wedge (Figures 9 and 10). In the models of the Manglares segment, the depth, width, and lateral distance from the trench axis to the oil and gas generation zone are doubled when compared to the results obtained in the northern Patía segment.

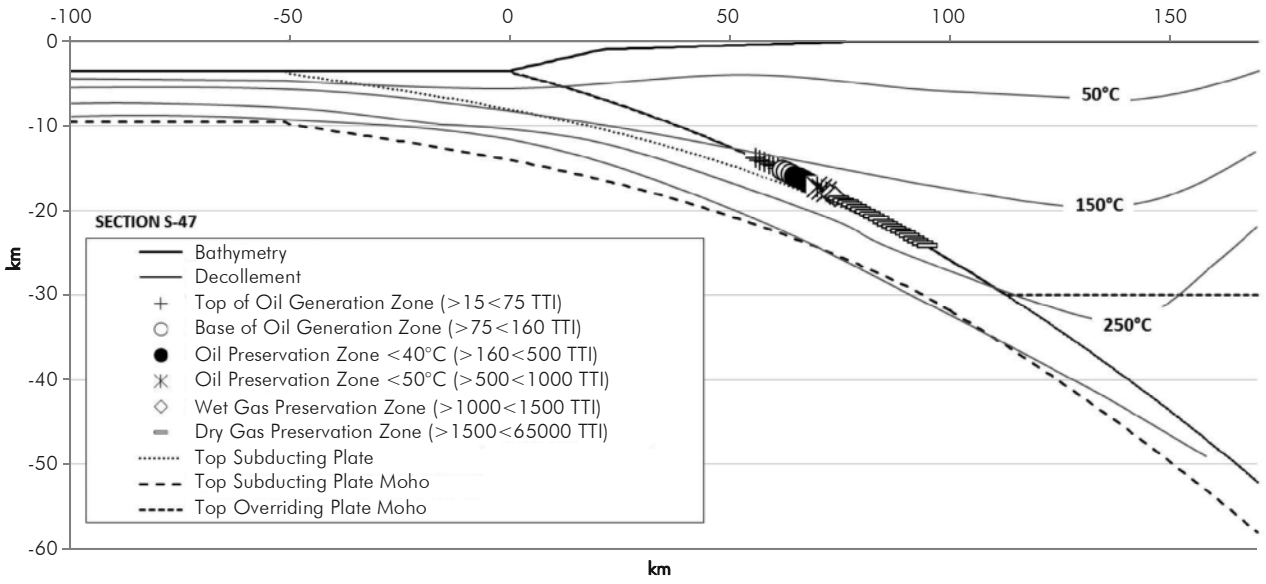

Figure 10. Present day hydrocarbon generation zones (oil and gas) as predicted by the 2D *TTIArr* modeling along the subduction zone in the section 3 (see location in the Figure 7). This section represents the structure of the margin between the Tumaco and Manglares segments. Vertical exaggeration = x 2.

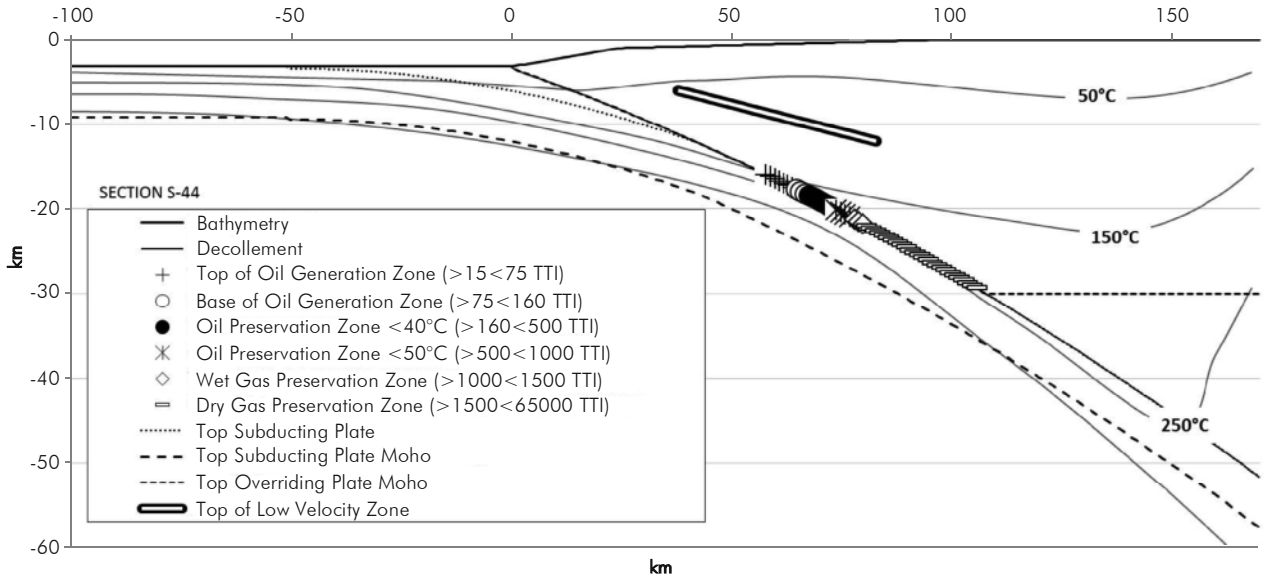

Figure 11. Present day hydrocarbon generation zones (oil and gas) as predicted by the 2D *TTIArr* modeling along the subduction zone in section 4 (see location in the Figure 7). Note the top of the Low Velocity Zone as defined by García – Cano et al. (2014) using 3D seismic refraction data in the Manglares segment is located up dip of the hydrocarbon generation zones.

The variation in location and breadth of the zones of hydrocarbon generation and preservation along the NESC margin could potentially derive from a number of variables including changes in the convergence rate along the margin, variations in the thermal regime and/or changes in the thickness of the subducting sediments. Along the Costa Rica margin, numerical models suggest that the depth and extent of the generation of hydrocarbons changes as a function of the rate of convergence and the thermal structure (Lutz *et al*. 2004). The GPS data suggest that the convergence rate between the plates of Nazca and South American decreases very slightly from by ~4 mm/y from South to North (Trenkamp *et al*. 2002). The variation in convergence rate along the NESC margin is probably too low to explain the changes in the distribution of hydrocarbon

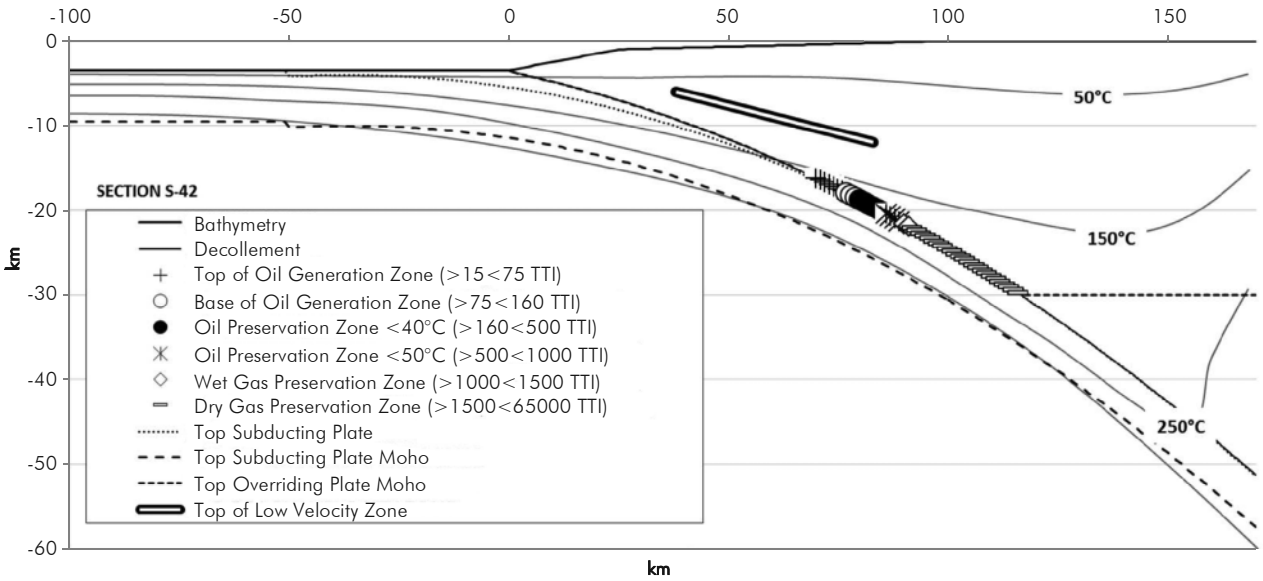

Figure 12. Current hydrocarbon generation zones (oil and gas) as predicted by the 2D *TTIArr* modeling along the subduction plane in Section 5 (see location in Figure 7). Note the top of the Low Velocity Zone as defined by García – Cano et al. (2014) using 3D seismic refraction data in the Manglares segment is located up dip of the hydrocarbon generation zones.

generation and preservation zones observed in the *TTIArr* modeling.

Heat flow data along the NESC margin illustrate important variations in thermal structure with high values of heat flow in the Patía segment (~100 mW/m^2), with lower values of heat flow (~75 mW/m^2) in the Manglares segment (Marcaillou *et al*. 2008; Marcaillou *et al*. 2006 a). The results of the *TTIArr* models reflect these lateral variations in the heat flow values, especially in the variable depth of the oil and gas windows and the changes in distance with respect to the trench axis. The *TTIArr* models located in the portions of the NESC with high heat flow values (Patía segment) indicate conditions for hydrocarbon generation in the upper levels of the subduction zone (<10 km depth) and near the trench axis. In contrast, the segments with low heat flow values (Manglares and Tumaco segments), exhibit conditions for hydrocarbon generation at greater depths within the subduction zone (> 10 km) and are located farther (>60 km) from the trench axis.

Bathymetric charts and seismic profiles suggest that the thickness of sediments accumulated over the Nazca plate have great lateral variations (< 2km in the Patía segment and > 5 km in the Manglares segment) (Collot *et al*., 2005). It is possible that the thermal segmentation of the NESC margin is related to the changes in the thickness of sediments undergoing subduction (Marcaillou *et al*. 2008; Marcaillou *et al*. 2006 a) and that the present day distribution of hydrocarbon generation zones along the top of the subducting slab are related to the thickness of the sediments undergoing subduction. An analysis of the width of the current hydrocarbon generation zones as defined by the *TTIArr* modeling versus the thickness of the sediments undergoing subduction provides insight into this relationship (Figure 13). The analysis suggests that an increased width of the hydrocarbon generation zones along the subduction plane is related to the variation of the thickness of the sediments undergoing subduction in the Patía and Tumaco segments (Sections S1 to S3) in a linear fashion (Figure 13). However, the width of the hydrocarbon generation zones in the Manglares segment (Sections S4 and 5) does not exhibit the linear relationship observed in the Patía and Tumaco segments (Figure 13). This anomalous width requires an additional mechanism to alter the thermal structure in the Manglares segment and expand the hydrocarbon generation zones along the top of the subducting plate.

As described in the regional tectonic setting, the Nazca Plate contains numerous rift, grabens, ridges, and transforms structures very close to the Manglares and Esmeraldas segments. The bathymetric and geophysical information show that the majority of these structures are sealed by sediments and separated from the trench in the Patía and Tumaco segments. However, in the Manglares segment, the Nazca Plate has numerous structures that are expressed on the present-day sea floor

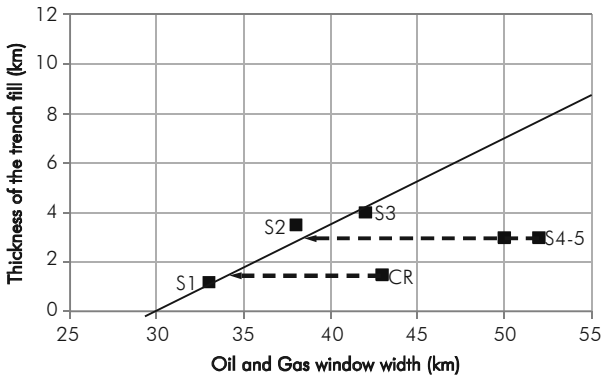

Figure 13. Thickness of the trench fill sediments undergoing subduction *versus* the oil and gas window width along the subduction zone of the five sections modeled in the NESC margin (Section 1: S1; Section 2: S2; Section 3: S3, Section 4: S4, Section 5: S5). For comparison purposes, data from the Costa Rica margin (CR) from Lutz et al (2004) is plotted. Note that the sections S1 to S3 (Patía and Tumaco segments) define a linear relationship showing that the sediment thickness in subduction zones constrains the width of the oil and gas windows, while sections S4, S5 and CR (Manglares segment and Costa Rica margin) are not congruent with this relationship and suggest an additional mechanism to explain the enhancement of the current oil and gas windows like hydrothermal circulation in the subducting plate. x-axis label should read 'Oil and Gas window width (km)'

(e.g. the Yaquina graben, fossil transform faults, and submarine ridges) close to the trench axis (Figure 2). In the Costa Rica margin, the highly faulted Nazca Plate improves hydrothermal circulation with transmission of ocean bottom water through zones in the upper basaltic basement with high permeability, resulting in highly suppressed temperatures deep into the subduction zone (Kummer and Spinelli, 2008; Langseth and Silver, 1996; Harris *et al*. 2010).

Comparing the results of the *TTIArr* models in the Manglares segment with the results obtained for Lutz *et al* (2004) in the Costa Rica margin, it is observed that the width of the hydrocarbon generation zones are congruent with the thickness of the sediments undergoing subduction (Figure 13). Both models are similar in terms of the tectonic setting (same incoming plate and oceanic nature of the overriding plate). It is possible that combined mechanism variations in the thickness of sediments being subducted and hydrothermal circulation in the subducting plate alter the thermal structure in the Manglares segment in a manner similar to the Costa Rica Margin. This additional hydrothermal circulation (cooling) causes the formation of widest- and deepest hydrocarbon zones along the top of the subducting plate in comparison with the Patía and Tumaco segments (Figure 13). The analysis of the *TTIArr* modeling along the NESC margin suggest that in subduction zones with unstructured or relatively smooth subducting plates, the depth and width of the hydrocarbon generation zones are constrained by the thickness of the sediments undergoing subduction (like Patía and Tumaco segments), while in subduction zones with incoming plates that are heavily faulted and with rugose basement, the distribution of the hydrocarbon generation zones are driven by the degree of hydrothermal circulation (like the Manglares segment and the Costa Rica Margin).

MMigration pathways, trapping areas and hydrocarbon seepage

Geochemical analysis of samples recovered by dredge and piston core to the west of the Manglares basin (Figure 4) indicates the presence of fluids, gas, and oil of thermogenic origin (Figures 5 and 6) near the accretionary wedge zone. In sections 1 to 3 (Patia and Tumaco segments) the sediments recovered in piston cores contain medium to high abundances of adiamandoids, and suggest high contributions of hydrocarbons in the recent sediments (seeps) (Figures 5, 6 and 7), along the trace of thrust faults that were developed below the Patía and Tumaco highs (Figure 14). Interpretation of wide offset seismic lines suggests that these thrust faults extend to depths up to 10 km (Marcaillou, 2003; López 2009), close to the zones of generation and preservation of hydrocarbons along the top of the subducting plate deduced from the *TTIArr* models (Figure 14). Consistent with this evidence, it is possible that the thrust faults of the accretionary wedge, in the Patía and Tumaco segments function as migration pathways for hydrocarbons that were generated along the top of the subducting plate, with migration distances of ~25 km or less to the current seeps on the sea floor (Figure 14).

In the Manglares segment, the seismic reflection and refraction profiles show a highly structured basement with thrust faults throught the overriding plate that are rooted in the basal detachment (Collot *et al*. 2008; Agudelo *et al*. 2009), very close to the zone of generation of hydrocarbons identified by the *TTIArr* modeling (Figure 15). In this segment, a few samples of sediments were recovered by piston core, close to the trace of the splay fault defined by Collot *et al* (2008). These samples show low concentrations of adiamandoids and suggest very small hydrocarbons concentrations in the recent sediments (Figure 6). However, over the trace of a splay fault in this area blocks of carbonate crust were recovered, rich in *Caliptogenas magnificus* (Figures 4

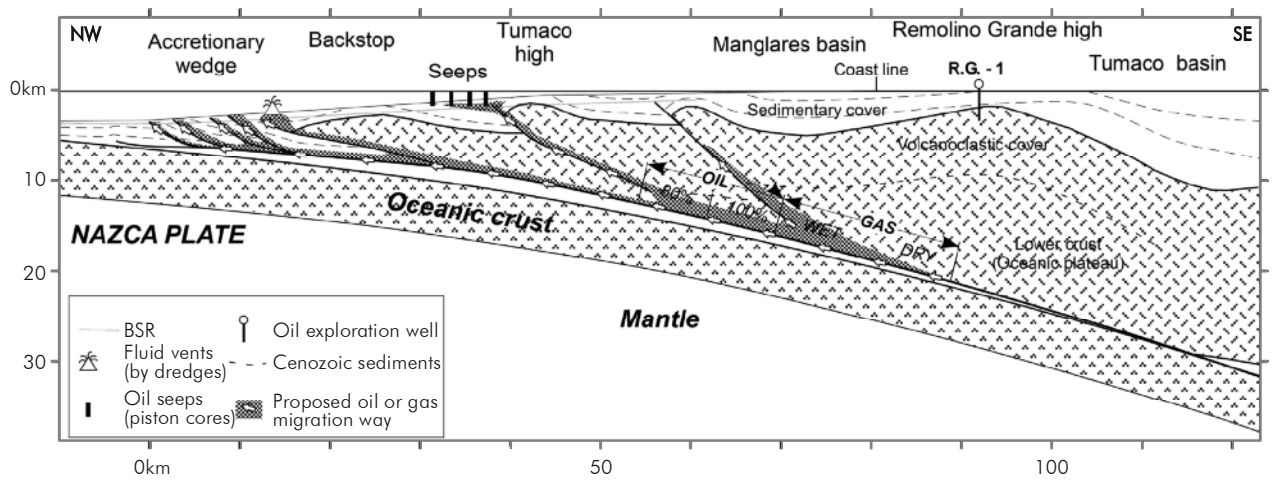

Figure 14. Representative cross-section (the location correspond with S-44 section in figure 7) of the crustal structure of the Patía and Tumaco segments (undergoing tectonic accretion), illustrating the double forearc basin system. The system comprises the Tumaco and Manglares basins, divided by the Remolino Grande high (after to Marcaillou et and Collot, 2008; Marcaillou et al. 2008, López, 2009). This forearc basin system is underlain by Mesozoic oceanic basement (drilled by the Remolino Grande – 1 well: RG-1) and bounded to the west by basement highs (Tumaco high). Note the occurrence of numerous basement involved thrust faults along the seaward border of the NESC margin that act as migration pathways between hydrocarbon generation zones along the top of the subducting plate (note the percent of hydrocarbon generated along the decollement) and areas on the seafloor that show evidence of thermogenic hydrocarbons such as the chemosynthetic communities (fluid vents) along the top of the accretionary wedge and oil seeps in sediments composing the backstop. Vertical exaggeration x1.

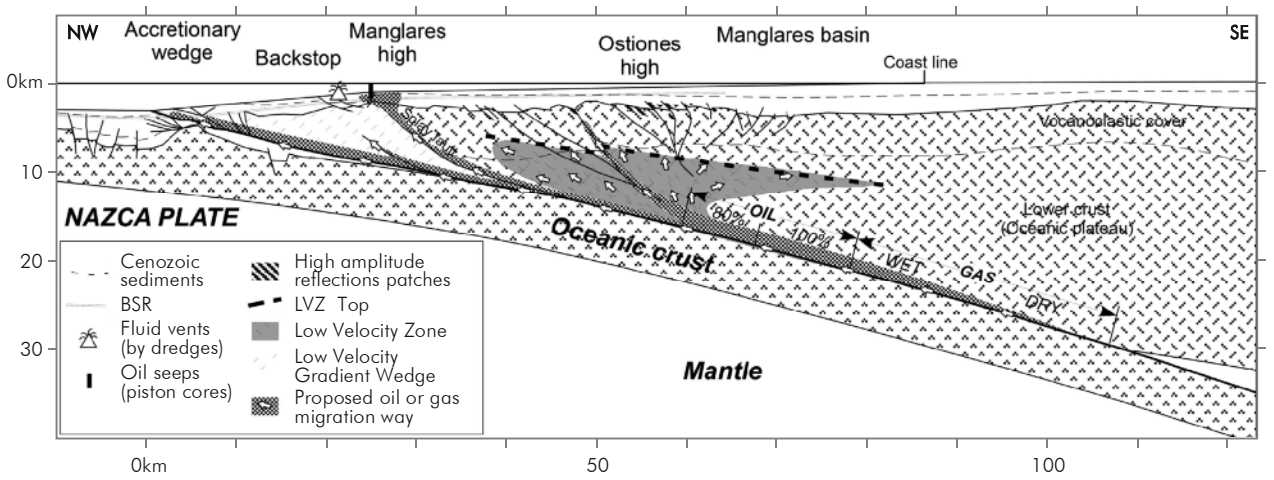

Figure 15. Representative cross-section (the location correspond to S-37 section in Figure 7) of the crustal structure of the Manglares segment (undergoing tectonic erosion), illustrating the Manglares basin that is locally divided by the Ostiones basement high (after to Collot et al. 2008). This forearc basin system was established over highly structured Mesozoic oceanic basement and is bounded to the west by the Manglares high. Note the location and extent of the LVZ and the LVGW near the splay fault (according to Collot et al. 2008; García – Cano et al. 2014), up dip from the current hydrocarbon generation zones along the subduction zone (note the percent of hydrocarbon generated along the decollement). The presence of fluid vents and oil seeps close to the splay fault trace at the seafloor suggest that this fault acts as a migration pathway, while high reflectivity patches over the LVZ and at the base of the sedimentary cover in the Manglares basin suggest potential areas of hydrocarbon trapping. Vertical exaggeration x1.

and 15), with isotopic ∂13C relationships that suggest a supply of gas or fluids from deeper thermogenic systems (Collot *et al*. 2005 a; López, 2009). This suggests that the splay fault is a migration pathway for thermogenic hydrocarbons and fluids generated along the basal detachment to the sea floor (Figures 4, 14 and 15). Nevertheless, according to the 3D seismic refraction results (Garcia-Cano *et al*., 2014), the East part of the low-velocity zone (~20 km of wide) is located immediately over the hydrocarbon generation zone of oil into the subduction plane, deduced by the *TTIArr* modelling (80 to 100 % of expulsion zones), while West part of the LVZ coincides with the root of basement faults (Figures 11, 12 and 15).

A key factor in the evolution of the LVZ in the Manglares segment is the increasing effect of the expelled fluids from the subducting sediments and the subsequent alteration of the overriding plate. Under this scenario, hydrocarbons generated along the decollement in the Manglares segment migrated up to the overriding plate with the other fluids resulting from the subduction and compaction/dewatering processes. During the alteration of the overriding plate, the migrating hydrocarbons were likely trapped in highly structured zones near the top of the LVZ or possibly migrated further up-dip to reservoirs and traps at the base of the Cenozoic sedimentary cover. The hydrocarbons trapped along the top of the LVZ could explain the formation of high reflectivity zones like unit G as described by Collot *et al*. (2008). In addition, hydrocarbons that migrated up to the base of the Cenozoic sedimentary cover could produce high reflectivity zones near basement involved faults (Figure 15).

In the Patía and Tumaco segments, the formation of the accretionary wedge drives the migration and trapping of the expelled fluids from the subducting sediments. In these segments, carbonate blocks similar to those recovered in the Manglares segment were recovered at two km below sea level (BSL) (Figure 4), close to the boundary between the oldest accretionary wedge and the basement backstop as defined by Marcaillou (2003). In this area, an analysis of the BSR and heat flow measurements shows high values of heat flow (up to 80 mW/m^2), near bathymetric valleys and may represent the trace of thrust faults that provide high permeability pathways for warm fluids to reach the seafloor (Collot *et al*. 2005b). Carbonate blocks were recovered close to the major thrust faults traces, supporting the role of these faults as migration pathways of warm fluids to the seafloor. We interpret the accretionary wedge in the Patía and Tumaco segments as being charged by thermogenic fluids, expelled from the sediments undergoing subduction. In this context the hydrocarbon that were produced along the subduction plane into the Patía and Tumaco segments could seep from levels deeper than 10 km, migrating through the accretionary wedge, and escaping to the seafloor thanks to faults and fractures, helping the formation of chemosynthetic communities (Figure 14).

The samples and heat flow measurements suggest the occurrence zones of fluids expulsion along the NESC margin. The origins of these zones of expulsion are poorly understudied and probably are important elements in the prediction of earthquake activities bearing in mind the process of fluid migration during interseismic periods (Doglioni *et al.* 2013). According to the model of behavior of fluids in compressive settings, hydrocarbons and other fluids are mainly expelled and preserved in overpressurized zones along the subduction plane during interseismic periods in the NESC margin. Later, during the coseismic periods these hydrocarbons migrate up to the overriding plate and into numerous features like LVZ, the accretionary wedge, the base of the sedimentary cover, or can filter up to the seafloor during the margin relaxation.

Petroleum system and exploratory plays

The essential elements of a petroleum system are the source rock, overburden rock, reservoir rock, and seal rock (Magoon and Beaumont 1999). This work provides the basis for defining the elements of a speculative petroleum system along the NESC margin. The occurrence of source rock is supported by samples of dredges and piston cores that were recovered during the AMADEUS Cruise (2005 a), that contain abundant fragments of plants into the accretionary wedge and submarine fan near the trench zone. These fragments of plants made part of sediments accumulated during events of extreme mass flow and turbidity current along the NESC margin (Ratzov, 2009). Sediments drilled by several ODP and DSDP legs along active continental margins in trench to slope transitions are rich in recycled vitrinite and reworked organic matter, caused by the erosion of sedimentary rocks in the forearc zone and transported by turbiditic currents into the deep ocean (Littke and Sachsenhofer, 1994). In the trench zone of the NESC margin, sediments transported by turbiditic currents probably began during the Pleistocene times covering distal turbidity sediments accumulated during the Pliocene times (Ratzov et.al, 2012). Taking into account our samples, the turbidity sedimentation, and the contents of organic matter observed in other convergent margins, we assume that the sediments undergoing subduction along the NESC margin have source rock potential with relatively sparse but constant fraction of organic matter (~1%), mainly composed of type II/III kerogens transported from the continent.

Burial history plots for the sediments of the NESC margin transported along the top of the Nazca Plate during the last 5 Myr, subduction initiated at 2.4 Ma, and the sediments entered into the oil generation window at

a depth of 11 km at ~1.1 Ma (Figure 16). The sediments reached the gas generation window at depths of ~15 km at 0.7 Ma (Figure 16). Taking into account the actual convergence rates along the NW South American margin, it is possible to consider that the sediments that enter in subduction along the NESC margin require from 1.1 to 1.6 Myr to reach the conditions of oil generation and from 1.65 to 2.1 Myr to reach the conditions of gas generation. The burial history plots suggest that the sediments included into the subduction zone of the Patia and Tumaco segments reach conditions favorable for the generation of oil and gas at depths more shallow than the sediments into the Manglares segment (Figure 14). This lateral variation in the oil and gas generation depth is consistent with the thermal segmentation of the margin reported by Marcaillou *et al* (2008), that constrains the distribution of the areas of oil and gas generation modelled along the top of the subducting plate (Figures. 8, 9, 10, 11, 12, 13).

Seismic refraction profiles show that velocities increase normally up to the basal detachment in the Patía and Tumaco segments (Agudelo, 2005), suggesting an unaltered and impermeable basaltic overriding plate over the areas of oil and gas generation that prevents the migration of hydrocarbons out of the subducting sediments into the hanging wall rocks (Figure 12). Nevertheless, geochemical analysis in samples of rocks and sediments suggests the presence of hydrocarbons that have migrated laterally along the faults that affect

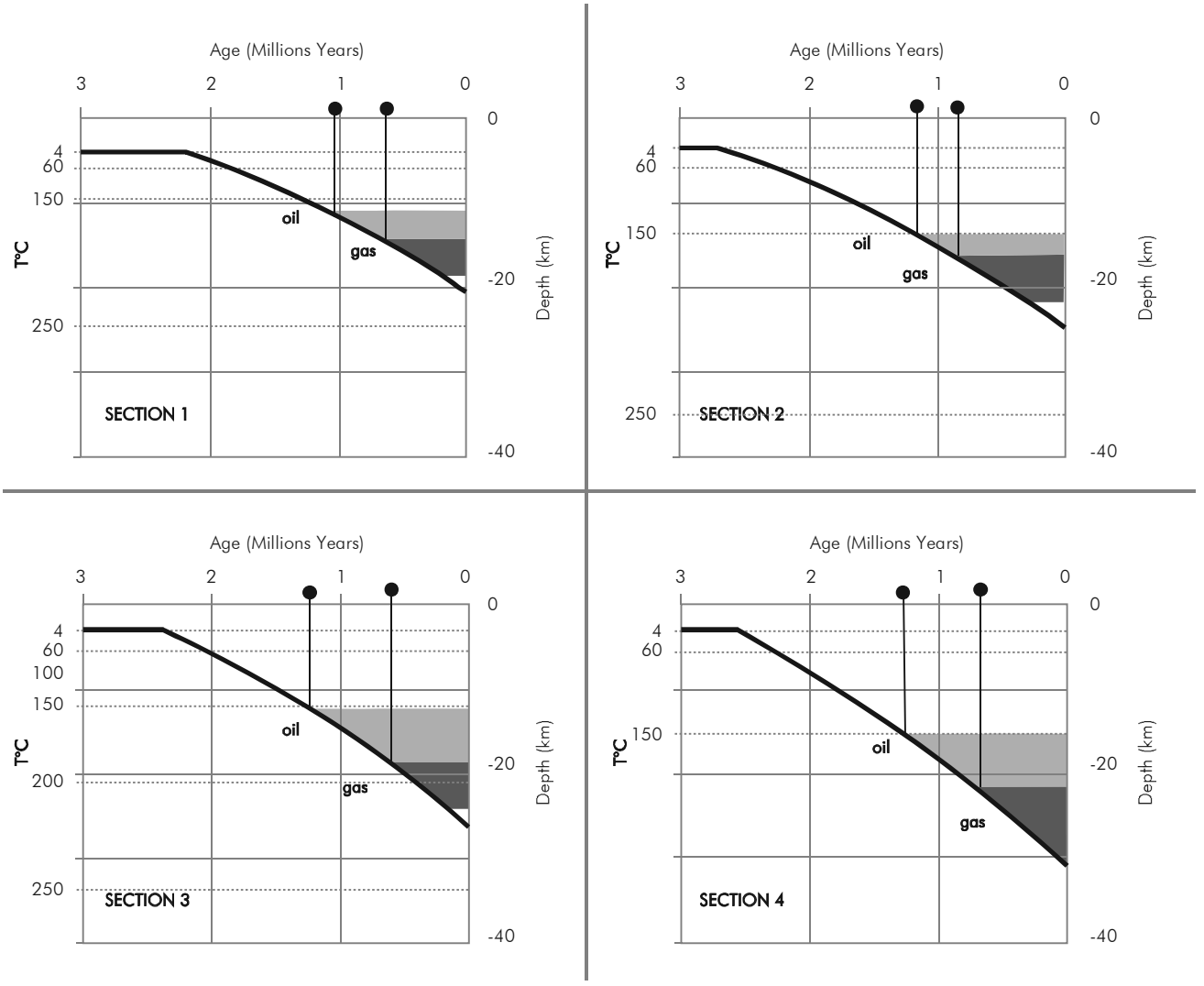

Figure 16. Burial history plots of the sediments at the top of the subducting plate from sections 1 to 4. Note the changes in the depth and the initiation of conditions of generation of oil and gas from the sediments in the Patía and Tumaco segments (sections 1 and 2 respectively) compared to the sections in the Manglares segment (sections 3 and 4). Black dots with vertical lines show the time at which oil and gas generation begins for each cross section.

the basement near the accretionary wedge, over the areas of oil and gas generation (Figure 5). While the upper part of the sediments involved in the subduction plane can act as an effective lateral migration pathway for fluids and gas of thermogenic origin (Tobin *et al*. 2001), it is possible that the decollement in the Patía and Tumaco segments acts as migration carrier bed up to the accretionary wedge, with some basement involved faults nearest to the subducting plate acting as migration pathways to the middle continental slope area (Figure 12). Reservoir properties are probably enhanced in the presence of the accretionary wedge thanks to the development of dense networks fractures observed in the rock samples of the Patía and Tumaco segments (Collot et.al, 2005). Seismic information shows several anticlines into the accretionary wedge and of the Patía and Tumaco segments with four way closures and closures against thrust faults, nevertheless, the thickness of the overburden and seal rocks are lower than 1 seg twt. In this scenario, we infer the greatest risk involves both overburden and seal rocks. This is consistent with fluid flux analysis in the accretionary wedges of the Alaskan Margin, the Nankai Trough, and the Barbados accretionary prism that show elevated rates of dewatering in the first 10 km of the accretionary wedge, which decrease progressively in the landward direction (von Huene *et al*. 1998; Saffer and Bekins, 1999). This landward decline in the fluid expulsion, favors the preservation of structures with the presence of seal rocks in bends of the subducting plate or subthrusting near the backstop boundary connected with the subducting plate migration pathways.

In the Manglares segment the degree of alteration of the overriding plate has encouraged the accumulation of hydrocarbons generated along the top of the subducting plate into the low velocity zone, sealed by the unaltered overlying oceanic basement (Figure 15). The progressive accumulation of hydrocarbons at the top of the low velocity zone is accompanied with other fluids expelled from the top of the subducting plate. This accumulation of fluids increases the reflectivity in seismic sequences that involve the basement like bright zones (e.g. Unit G of Collot *et al*., 2008) or migrate through overlying faults into the Cenozoic sedimentary cover (Figure 15).

The 2D modelling conducted in this study, coupled with available geochemical and geophysical studies allows us to suggest the presence of a potential petroleum system in the Manglares segment. The age of the reservoir rock is Neogene (age of the LVZ formation). Based on the piston core evidence, the Neogene sediments provided by the submarine fans systems along the trench is the source rock. The absence of positive oil-source rock correlation indicates a speculative petroleum system proposed as *Sediments in subduction* – LVZ ?. An analog of this petroleum system is the Costa Rica margin (affected by tectonic erosion), where a LVZ (DeShon *et al*. 2006) is located just above the hydrocarbon generation zones along the decollment as proposed by Lutz *et al* (2004). Thanks to these similarities, we interpret that such a petroleum system may occur in other convergent margins with oceanic overriding plates undergoing tectonic erosion processes, such as the Circum-Caribbean deformed belt, Nicaragua, Chile or Aleutians Islands.

4. CONCLUSIONS

- The results of the *TTIArr* modelling along the NESC margin show that the sediments located near the top of the subducting Nazca plate are currently under favorable conditions for thermogenic oil and gas generation at depths greater than 10 km. The models suggest that the variability in widths of the zones of hydrocarbon generation along the subduction zone are related to the changes in sediment thickness undergoing subduction in the Patía and Tumaco segments. However, in the Manglares segment, the zones of hydrocarbon generation are wider and deeper in comparison with the other segments and appear to have no relationship with the thickness of sediments undergoing subduction.

- We suggest that in subduction zones associated with unstructured or relatively smooth down-going plates, the depth and width of the hydrocarbon generation zones are controlled by the thickness of the sediments undergoing subduction (like the Patía and Tumaco segments). In subduction zones with down-going plates that are highly faulted and rugose, the distribution of the hydrocarbon generation zones is driven by the degree of hydrothermal circulation occuring in the subducting plate (e.g. the Manglares segment and the Costa Rica margin). Our interpretation of the geochemical and geophysical data suggest that thrust faults in the basement of the NESC margin act as

migration pathways for hydrocarbons generated along the decollement with lateral migration distances of ~25 km between the hydrocarbon generation zones and the occurences of seeps on the seafloor.

- In the Manglares segment (undergoing tectonic erosion), the hydrocarbons generated along the top of the subducting plate tends to migrate vertically to the overriding plate with other fluids expelled during the subduction process. These fluids are trapped in highly structured zones at the top of a LVZ, corresponding with high reflectivity zones imaged on seismic reflection profiles. Minor amounts of hydrocarbons continue their migration up to sedimentary reservoirs and traps into the base of the Cenozoic sedimentary cover, and produce high reflectivity zones proximal to basement faults. In the Tumaco and Patía segments, the majority of the hydrocarbons generated along the top of the subducting plate migrate up through the accretionary wedge, escaping into the seafloor through the faults and fractures, leading to the formation of chemosynthetic communities. Additionally, earthquake activity allows the migration of fluid from the decollement through basement involved thrust faults to traps in the low velocity zone or seeps on seafloor during periods of margin relaxation.

- The geophysical data and the proposed migration pathways of fluids in the NESC margin suggest that in segments affected by tectonic accretion there are problems in the preservation and quality of seal and traps in the accretionary wedge. Nevertheless, in areas of underplating below the basement of the backstop, the unaltered basement of the overriding plate has good sealing properties to hinder a greater migration of hydrocarbons generated along the top of the subducting plate.

- In segments of the margin affected by tectonic erosion, the low velocity zone defines a region that may have good properties to trap hydrocarbons and fluids expelled from the subduction zone defining a speculative petroleum system consisting of sediments undergoing subduction (source rock) and the low velocity zone (reservoir and trap). A possible analogy for this speculative petroleum system occurs in the Costa Rica area and may be extended to other convergent margins like Nicaragua, Chile, Aleutians Islands or Southern Caribbean deformed belt.

ACKNOWLEDGEMENTS

We are grateful to the Institut de Recherche pour le Développement (IRD) for funding and providing access to AMADEUS cruise samples and reports, ECOPETROL for providing access to piston core descriptions and geochemical results along the Western Colombia margin. We especially thank the anonymous reviewers and the editorial Committee of CT&F by the patient review, correction and recommendations to improve the content and form of this work.

REFERENCES

Agudelo, W., Ribodetti, A., Collot, J.-Y., and Operto, S., 2009. Joint inversion of multichannel seismic reflection and wide-angle seismic data: Improved imaging and refined velocity model of the crustal structure of the north Ecuador–south Colombia convergent margin. Journal of Geophysical Research, V. 114, pages 1 - 27.

Agudelo, W., 2005. Imagerie sismique quantitative de la marge convergente d'Equateur- Colombie: Application des méthodes tomographiques aux données de sismique réflexion multitrace et réfraction-réflexion grand-angle des campagnes SISTEUR et SALIERI. Thèse de doctorat de l'Université Paris 6. 203 p.

ANH, 2014. Pacific Margin – Pacific Basins: presentation. In: RONDA COLOMBIA 2014. Bogotá, p. 84.

Areshev, E. and Balayuk, I., 2006. Unique potentialities of hydrocarbon deposits formation in subduction zones. Geophysical Research Abstracts, Vol. 8, 00450.

Aspden, J. A., and Litherland, M., 1992. The geology and Mesozoic collisional history of the Cordillera Real, Ecuador. Tectonophysics, Vol. 205, pages 187-204.

Barrero, 1979. Geology of the central Western Cordillera west of Buga and Roldanillo, Colombia. Publicación Geológica Especial del INGEOMINAS, n°4, 75 p.

Beck, S. L., and L. J. Ruff (1984), The rupture process of the great 1979 Colombia earthquake: Evidence for the asperity model, J. Geophys. Res., 89, 9281– 9291.

Behrmann, J. H., Lewis, S. D., Musgrave, R. J., *et al*., 1992. Proceedings of the Ocean Drilling Program, Initial reports,

Vol. 141: College Station, TX (Ocean Drilling Program). Sites 859 - 863, pages 75 – 446.

Calahorrano, A., Sallarès, V., Collot, J.-Y., Sage, F. and Ranero, C., 2008. Nonlinear variations of the physical properties along the southern Ecuador subduction channel: Results from depth-migrated seismic data. Earth and Planetary Science Letters 267, pages 453 – 467.

Case, J. E., Barnes, J., Paris, G., Gonzalez, I. H., and Viña, A., 1973. Trans Andean Geophysical profile, Southern Colombia. Geological Society of America, v. 84, pages 2895 – 2904.

Cediel, F., R. P. Shaw, and C. Caceres, 2003, Tectonic assembly of the Northern Andean Block, in C. Bartolini, R. T. Buffler, and J. Blickwede, eds., The Circum-Gulf of Mexico and the Caribbean: Hydrocarbon habitats, basin formation, and plate tectonics: AAPG Memoir 79, pages 815– 848.

Cediel F., Restrepo I., Marín-Cerón M.I., Duque-Caro H., Cuartas C., Mora C., Montenegro G., García E., Tovar D., Muñoz G., 2009. Geology and Hydrocarbon Potential, Atrato and San Juan Basins, Chocó (Panamá) Arc. Tumaco Basin (Pacific Realm), Colombia. 171 pages.

Christeson, G. L., McIntosh, K. D., and Shipley, T. H., 1999. Structure of the Costa Rica convergent margin, offshore Nicoya Peninsula. Journal of Geophysical Research, Vol. 104, N° B11, pages 25443 – 25468. This article is not in the correct alphabetical position

Collot, J. – Y., Michaud, F., Alvarado, A., Marcaillou, B., Sosson, M., Ratzov, G., Migeon, S., Calahorrano, A., y Pazmiño, A., 2009. Visión general de la morfología submarina del margen convergente de Ecuador – Sur de Colombia: implicaciones sobre la transferencia de masa y la edad de la subducción de la Cordillera de Carnegie. *In J.* – I. Collot, V. Sallarès y N. Pazmiño Edts. Geología y geofísica marina y terrestre del Ecuador. Pages 47 – 74.

Collot, J.-Y., Agudelo, W., Ribodetti, A. and Marcaillou, B., 2008. Origin of a crustal splay fault and its relation to the seismogenic zone and underplating at the erosional north Ecuador–south Colombia oceanic margin. Journal of Geophysical Research, V. 113, 19 p.

Collot J-Y, Alvarado, A., Dumont, J-F., Eissen, J-P., Joanne, C., Lebrun, J-F., Legonidec, Y., Lewis, T., Lopez, E., Marcaillou, B., Martinez, I., Michaud, F., Migeon, S., Oggian, G., Pazmiño, A., Santana, E., Schneider, J-L., Sosson, M., Spence, G., Toro, A., Wada I., 2005 a. The AMADEUS cruise Ecuador-Colombia Feb 4th – March 9th 2005 a. Preliminary report (unpublished). 327 p.

Collot, J. – Y., Migeon, S., Spence, G., Legonidec, Y., Marcaillou, B., Schneider, J.-L., Michaud, F., Alvarado, A., Lebrun, J.-F., Sosson, M. And Pazmiño, A., 2005 b. Seafloor margin map helps in understanding subduction Earthquakes. EOS, v. 86, n° 46, p. 463 – 465.

Collot, J – Y., Marcaillou, B., Sage, F., Michaud, F., Agudelo, W., Charvis, P., Graindorge, D., Gutscher, M. – A. and Spence, G., 2004. Are rupture zone limits of great subduction earthquakes controlled by upper plate structures? Evidence from multichannel seismic reflection data acquired across the northern Ecuador southwest Colombia margin. Journal of Geophysical Research, Vol. 109, pages 1 – 14

Daly, M. C., 1989. Correlations between Nazca/Farallon plate kinematics and forearc basin evolution in Ecuador. Tectonics, v. 8, n° 4, pp. 769 – 790.

DeShon, H. R., Schwartz, S. Y., Newman, A. V., González, V., Protti, M., Dorman, L. M., Dixon, T. H., Sampson, D. E. and Flueh, E. R., 2006. Seismogenic zone structure beneath the Nicoya Peninsula, Costa Rica, from three-dimensional local earthquake P- and S-wave tomography. Geophysical Journal International, 164, pages 109 – 124.

Dessa, J.-X., Operto, S., Kodaira, S., Nakanishi, A., Pascal, G., and Virieux, J., 2004. Multiscale seismic imaging of the Eastern Nankai trough by full wave inversion. Geophysical Research Letters, Vol. 31, 4 pages.

Doglioni, C. Barba, S., Carminati, E. and Riguzzi, F., 2013. Fault on-off versus coseismic fluids reaction. Geosciences Frontiers, http://dx.doi.org/ 10.1016/j.gsf.2013.08.004

Echeverria, L. M., 1980. Tertiary or Mesozoic Komatiites from Gorgona Island, Colombia: Field Relations and Geochemistry. Contributions to Mineralogy and Petrology, 73, p. 253 – 266.

Evans, C. D. R., and Whittaker, J. E., 1982. The geology of the Western part of the Borbón Basin, Northwest Ecuador, in Trench – forearc geology, edited by J. K. Leggett, Geological Society of London Special Publication, 10, p. 191 – 198.

Gansser, A., 1950. – Geological and petrological notes on Gorgona Island in relation to North-Western South America, Bull Suisse de Min. et Pet., vol. 30, pp. 219-237, 6 fig., 4 pl., 2 maps, Bern.

Garcia – Cano, L. C., Galve, A., Charvis, P. and Marcaillou B., 2014. Three-dimensional velocity structure of the outer fore arc of the Colombia-Ecuador subduction zone and implications for the 1958 megathrust earthquake rupture zone. Journal of Geophysical Research, Solid Earth, Vol. 119, Issue 2, pages 1041 - 1060

Hardy, N. C., 1991, Tectonic evolution of the eastern most Panama basin: some new data and inferences. Journal of South American Earth Sciences, v. 4, n° 3, pages 261 – 269.

Harris, R. N., Spinelli, G., Ranero, C. R., Grevemeyer, I., Villinger, H. and Barkhausen, U. 2010. Thermal regime of the Costa Rican convergent margin: 2. Thermal models of the shallow Middle America subduction zone offshore Costa Rica. Geochemistry, Geophysics and Geosystems, Vol. 11, Number 12, 22 pages.

Hensen, C., Wallmann, K., Schmidt, M., Ranero, C. R. and Suess, E., 2004. Fluid expulsion related to mud extrusion off Costa Rica – A window to subducting slab. Geology, Vol. 32, N° 3, pages 201 – 204.

Hunt, J. M., Lewan, M. D., and Hennet, R. J. – C., 1991. Modeling Oil Generation with Time – Temperature Index Graphs Based on the Arrhenius Equation. AAPG Bulletin, Vol. 75, n° 4, pages 795 – 807.

Hunt, J. M. and Hennet, R. J., 1992. Modelling Petroleum Generation in Sedimentary Basins. In: Organic matter, productivity, accumulation and preservation in recent and ancient sediments. Edited by: Jean Whelan and John W. Farrington. Columbia University Press, N.Y. Oxford. p. 20 – 51.

Hyndman, R. D., and Peacock, S. M., 2003, Serpentinization of the forearc mantle. Earth and Planetary Science Letters, 212, p. 417 – 432.

Jeffrey, A. W. A., Pflaum, R. C., McDonald, T. J., Brooks, J. M., 1982. Isotopic analysis of core gases at sites 565-570, deep sea drilling project Leg 84. Initial reports of the Deep Sea Drilling Project: Washington, DC,US Gov't. Printing Office, Volume 84, DSDP 84, pages 719 – 726.

Jones, V. t., and Drozd, R. J., 1983. Predictions of oil or gas potential by near-surface geochemistry. AAPG, v67, No. 6, p. 932-952

Kanamori, H., and K. C. McNally (1982), Variable rupture mode of the subduction zone along the Ecuador-Colombia coast, Bull. Seismol. Soc. Am., 72(4), 1241–1253

Kelleher, J. (1972), Rupture zones of large South American earthquakes and some predictions, J. Geophys. Res., 77, 2087–2103.

Kerr, A. C., Aspden, J. A., Tarney, J., and Pilatasig L., F., 2002. The nature and provenance of accreted oceanic terrains in Western Ecuador: geochemical and tectonic constrains. Journal of the Geological Society, London, v. 159, p. 577 – 594.

Kendrick, E., Bevis, M., Smalley Jr., R., Brooks, B., Barriga Vargas, R., Lauria, E., Souto Fortes, L. P., 2003. The Nazca–South America Euler vector and its rate of change. Journal of South American Earth Sciences, v. 16, pages 125–131.

Kimura, G., Silver, E.A., Blum, P., *et al*., 1997. Proceedings of the Ocean Drilling Program, Initial reports, Vol. 170: College Station, TX (Ocean Drilling Program). Sites 1040 - 1043, pages 95 – 213.

Kodaira, S., Iidaka, T., Nakanishi, A., Park, J. O., Iwasaki, T. and Kaneda, Y., 2005. Onshore – offshore seismic transect from eastern Nankai Trough to central Japan crossing a zone of the Tokai slow slip event. Earth Planets Space, N° 57, pages 943 - 959

Kummer, T., and Spinelli, G. A., 2008. Hydrothermal circulation in subducting crust reduces subduction zone temperatures. Geology, v. 36, no. 1, pages 91 – 94.

Kvenvolden, K. A. and von Huene, R., 1985. Natural gas generation in sediments of the convergent margin of the Eastern Aleutian trench area, in D. G. Howell ed., Tectonostratigraphic terrains of the Circum-Pacific region, V.1, pages 31 – 49.

Langseth, M. G. and Silver, E. A., 1996. The Nicoya convergent margin – a region of exceptionally low heat flow. Geophysical Research Letters, Vol. 23, No. 8, Pages 891 – 894.

Littke, R., and Sachsenhofer, R. F., 1994. Organic Petrology of Deep Sea Sediments: A Compilation of Results from the Ocean Drilling Program and the Deep Sea Drilling Project. Energy & Fuels, Vol. 8, No. 6, pages 1448 - 1512

Lonsdale, P. and Klitgord, K. D., 1978. Structure and tectonic history of the eastern Panama basin. GSA Bulletin, v. 89, pages 981 – 999.

Lonsdale, P., 2005. Creation of the Cocos and Nazca plates by fission of the Farallon plate. Tectonophysics, 404, pages 237 – 264.

López E., 2009. Evolution tectono – stratigraphique du double basin avant – arc de la marge convergente Sud – Colombienne – Nord Equatorienne pendant le Cénozoïque. Thèse de Doctorat de l'Université de Nice Sophia Antipolis. 369 p.

Lutz, R., Littke, R., Gerling, P. and Bönnemann, C., 2004. 2D numerical modeling of hydrocarbon generation in subducted sediments at active continental margin of Costa Rica. Marine and Petroleum Geology 21, pages. 753 – 766.

Luzieux L. D. A., Heller F., Spikings R., Vallejo C. F., and Winkler W., 2006. Origin and Cretaceous tectonic history of the coastal Ecuadorian forearc between 1°N and 3°S: Paleomagnetic, radiometric and fossil evidence. Earth and Planetary Sciences and Letters 249, p 400 – 414.

Magoon, L. B., and Beaumont, E. A., 1999. Petroleum system (chapter 3). In Exploring for Oil and Gas Traps, Edward A. Beaumont and Norman H. Foster, eds., Treatise of Petroleum Geology, Handbook of Petroleum Geology. pp. 34

Manchuel, K., Régnier, M., Béthoux, N., Font, Y., Sallarès, V., Díaz, J. and Yepes, H., 2011. New insights on the interseismic active deformation along the North Ecuadorian–South Colombian (NESC) margin. Tectonics, Vol. 30, Issue 4, pages 1 - 25.

Marcaillou, B. and Collot, J. – Y., 2008, Chronostratigraphy and tectonic deformation of the North Ecuadorian – South Colombian offshore Manglares forearc basin. Marine Geology, n° 255, pages 30 – 44.

Marcaillou, B., Spence, G., Wang, K., Collot, J.-Y. and Ribodetti, A., 2008. Thermal segmentation along the N. Ecuador – S. Colombia margin (1 – 4°N): Prominent influence of sedimentation rate in the trench. Earth and Planetary Sciences and Letters, 272, pages 296 – 308.

Marcaillou, B., Spence, G.D., Collot, J.Y., Wang, K., 2006 a. Thermal regime from bottom simulating reflectors along the N Ecuador–S Colombia margin: relation to margin segmentation and the twentieth century great subduction earthquakes. Journal of Geophysical Research. 111. doi:10.1029/2005JB004239.

Marcaillou, B., Charvis, P. and Collot, J. – I., 2006 b. Structure of the Malpelo Ridge (Colombia) from seismic and gravity modelling. Marine Geophysical Research. 14 p.

Marcaillou, B., 2003. Régimes tectoniques et thermiques de la marge Nord Equateur – Sud Colombie (0° - 3,5°N° - Implications sur la sismogènese. thèse Ph.D., Université Pierre et Marie Curie, Paris. 197 p., 10 annexes.

McCourt, W. J., Aspden J. A., Brook M., 1984. New geological and geochronological data from the Colombian Andes: continental growth by multiple accretion. Journal of Geological Society, London, v. 141, pages 831 – 845.

Meissnar, R. O., Flueh, E. R., Stibane, F. and Berg, E., 1976. Dynamics of the active plate boundary in southwest Colombia according to recent geophysical measurements: Tectonophysics, Vol. 35, pages 115 – 136.

Meschede, M., and Barckhausen, U., 2000. Plate tectonic evolution of the Cocos-Nazca spreading center. In Silver, E.A., Kimura, G., and Shipley, T.H. (Eds.), Proc. ODP, Sci. Results, 170: College Station, TX (Ocean Drilling Program), pages 1–10

Meyer, R. P., Mooney, W. D., Hales, A. L., Hesley, C. E., Wollar, G. P., Hussong, D. M., Ramirez, J. E., 1977. Refraction observations across the leading edge, Malpelo Island to the Colombian Cordillera Occidental. In J. E. Ramirez and L. T. Aldrich Eds., The ocean – land transition in the southwest Colombia. Instituto Geofísico – Universidad Javeriana, Bogota, Colombia, pages 83 – 136.

Mountney, N. P., and Westbrook, G. K., 1996, Modelling sedimentation in ocean trenches: The Nankai Trough from 1 Ma to present: Basin Research, v. 8, pages 85–101.

Pardo – Casas, F., and Molnar, P., 1987. Relative motion of the Nazca (Farallon) and South American plates since Late Cretaceous time. Tectonics, v. 6, n° 3, pages 233 – 248.

Ranero, C. R., and R. von Huene, 2000. Subduction erosion along the Middle America convergent margin, Nature, 404, 748– 752.

Ratzov, G. 2009. Processus gravitaires sous-marins le long de la zone de subduction Nord-Equateur-Sud Colombie: Apports à la connaissance de l'érosion tectonique et de la déformation d'une marge active. Implications sur l'aléa tsunamis. Thèse de Doctorat de l'Université de Nice – Sophia Antipolis. 217 p.

Ratzov, G., Sosson, M., Collot, J-Y., and Migeon, S., 2012. Late Quaternary geomorphologic evolution of submarine canyons as a marker of active deformation on convergent margins: The example of the South Colombian margin. Marine Geology, 315-318, pp 77 – 97.

Reynaud, C., Jaillard, E., Lapierre, H., Mamberti, M., and Mascle, G. H., 1999. Ocean plateau and island arc of southwestern Ecuador: their place in the geodynamic evolution of northwestern South America. Tectonophysics, 307, p. 235 – 254.

Saffer, D. M. and Bekins, B. A., 1999. Fluid budgets at convergent plate margins: Implications for the extend and duration of fault zone dilation. Geology, Vol. 27, N° 12, pages 1095 – 1098.

Sage, F., Collot, J.-Y. and Ranero, C. R., 2006. Interplate patchiness and subduction erosion mechanism: evidence from depth-migrated seismic images at the central Ecuador convergent margin. Geology, v. 34, n° 12, pages 997 – 1000.

Sallarès, V. and Ranero, C. R., 2005. Structure and tectonics of the erosional convergent margin off Antofagasta, north Chile (23°30'S). Journal of Geophysical Research, Vol. 10, B06101, 19 p.

Spadea, P. and Spinosa, A., 1986. Petrology and chemistry of late Cretaceous volcanic rocks from the southernmost segment of the Western Cordillera of Colombia (South America). Journal of South American Earth Sciences, v. 9, n 1/2, pages 79 – 90.

Taira, A., Hill, I., Firth, J., *et al*., 1991. Proceedings of the Ocean Drilling Program, Initial reports, Vol. 131: College Station, TX (Ocean Drilling Program). Site 808, pages 71 – 269.

Trenkamp, R., Kellogg, J. N., Freymueller, J. T., and Mora, H., 2002. Wide plate margin deformation, southern Central America and northwestern South America, CASA GPS observations, J.S. Am. Earth Sci. 15, pages 157 - 171.

Tobin, H., Vannucchi, P. and Meschede, M., 2001. Structure, inferred mechanical properties, and implications for fluid transport in the decollement zone, Costa Rica convergent margin. Geology, Vol. 29, N° 10, pages 907 – 910.

von Huene, R., *et al*., 1977. Initial reports of the Deep Sea Drilling Project: Washington, DC, US Gov't. Printing Office, Volume 57, Site 441, pages 319 – 354.

von Huene, R., *et al*., 1982. Initial reports of the Deep Sea Drilling Project: Washington, DC,US Gov't. Printing Office, Volume 84, Site 566, pages 79 – 109.

von Huene, R., Klerchen, D., Gutscher, M. and Fruehn, J., 1998. Mass and fluid flux during accretion at the Alaskan margin. Geological Society of America Bulletin, Vol. 110, N° 4, pages 468 – 482.

von Huene, R., Ranero, C. R., and Vannucchi, P., 2004. Generic model of subduction erosion. Geology, v. 23, no 10, pages 913 - 916

Waples, D. W., 1980. Time and temperature in petroleum formation: application of Lopatin's method to petroleum exploration. AAPG Bulletin, v. 64, n° 6, p. 916 – 926.

Watkins, J. S., *et al*., 1981. Initial reports of the Deep Sea Drilling Project: Washington, DC,US Gov't. Printing Office, Volume 66, Site 489, pages 107 – 150.

Westbrook, G. K., Carson, B., Musgrave, R. J., *et al*., 1994, Proceedings of the Ocean Drilling Program, Initial reports, Vol. 146 (Part I): College Station, TX (Ocean Drilling Program). Sites 889 - 892, pages 127 – 378.

Wood, D. A., 1988. Relationships between thermal maturity indices calculated using Arrhenius equation and Lopatin method: implications for petroleum exploration: AAPG Bulletin, v. 72, pages 115 – 134.

AUTHORS

Eduardo López-Ramos
Affiliation: *ECOPETROL S.A*

Vicepresidencia de Exploración – *Gerencia Offshore*
Geologist, *Universidad Nacional de Colombia*
M.Sc. Earth Sciences *Universidad Nacional de Colombia*
Ph.D. Sciences de la Terre, *et l'Universe, Université de Nice – Sophia Antipolis (France)*
e-mail: eduardo.lopezra@ecopetrol.com.co